The Proactive Network Maintenance Comeback

OFDM and OFDMA Bring New, Laser-Guided Precision for Plant Fault Distancing

A technical paper prepared for presentation at SCTE TechExpo24

Larry Wolcott
Engineering Fellow
Comcast Corporation
Larry_Wolcott@cable.comcast.com

Jason Rupe
Principal Architect
CableLabs
j.rupe@cablelabs.com

Tom Kolze
R & D Advanced Technology Development Engineer
Broadcom
tom.kolze@broadcom.com

Alexander (Shony) Podarevsky
Architect and Technical Leader
Promptlink Communications, Inc
shony@promptlink.com

Mike Spaulding
Vice President, Plant Maintenance
Comcast Corporation
Michael_Spaulding@cable.comcast.com

Table of Contents

Title **Page Number**

List of Figures

Title **Page Number**

1. Introduction

Proactive network maintenance (PNM) has been a cornerstone in detecting and locating faults in cable and plant infrastructure since 2009. Despite its long history, the deployment of downstream (DS) orthogonal frequency-division multiplexing (OFDM) and upstream (US) orthogonal frequency-division multiple access (OFDMA) technologies bring revolutionary enhancements over legacy single carrier quadrature amplitude modulation (SC-QAM) channels which use 24-tap pre-equalizers (Pre-EQ) in the upstream. The introduction of 25 kilohertz (kHz) and 50 kHz subcarrier spacing, along with a significantly wider channel width and higher sample rates, dramatically improves resolution and sensitivity. This advancement enables the precise location of damaged cable faults to within just a few feet.

In the 2021 Society of Cable Telecommunications Engineers (SCTE) paper, "OFDMA Predistortion Coefficient and OFDM Channel Estimation Decoding and Analysis" [1], the authors of the paper were right. With the introduction of OFDM and OFDMA in the DOCSIS® 3.1 specification, channel estimation coefficients and pre-equalization telemetry respectively become increasingly important. They provide high-resolution information useful for troubleshooting the cable plant: "This wider bandwidth provides high-resolution time responses, enabling cable problems to be identified with high accuracy." While these data elements from the PNM catalog have been known and used for over a decade, an individual SC-QAM channel was too narrow of a frequency band to provide detailed information. Operators employed some methods that used the information from SC-QAM signals to interpolate coarse responses in channel estimation and pre-equalization data, thus approximating the information from a wider frequency. However, these approaches were less accurate than the capabilities offered by DOCSIS 3.1. Fault localization and repair still require digging, but with DOCSIS 3.1 technology, localization can be done with greater precision. As Tom Williams put it, "dig a hole, not a trench." Instead of just eight or 24 complex values of data, we get many times more.

Thankfully, the paper's authors also outlined the process by which one can remove unwanted components from the telemetry to provide a clean view of reflected energy in the time domain, thus revealing details about the plant between the node and the cable modem (CM). A clear view of the signal can be found by removing a linear phase delay component from the data, converting to the time domain, correcting the phase data by adjusting the phase at time zero to be zero, then transforming to the frequency domain (FD) for comparisons.

This paper presents an in-depth analysis of actual plant conditions, demonstrating that leaks, ingress points, cracked cables, and damaged drops can no longer evade the laser-like precision of this new high-resolution PNM analysis. The paper guides readers through the entire process of collecting, decoding, and analyzing PNM data, including a simplified approach to Tom Williams's OFDM phase correction routine.

2. Background

Impedance mismatches cause reflections in a transmission line, such as a coaxial cable. Reflected waves will interact with the incident wave, producing a distribution of fields along the transmission line, known as standing waves. The presence of two or more reflections in a transmission line can result in amplitude ripple in the frequency response. While the term "standing wave" is often used to describe amplitude ripple, they are not the same. A standing wave exists in the radio frequency (RF) signal along the transmission line, while amplitude ripple describes the plot of amplitude data of the frequency response at a particular location, such as the input to a cable modem.

Amplitude ripple can indicate an RF impairment but can also exist in healthy cable systems caused by normal imperfections in the impedance characteristics found therein. Consider a scenario in which two

impedance mismatches exist in the coax part of the plant – say, the output of an amplifier and a water-filled tap some distance downstream from the amplifier. In the downstream, energy reflects off the second impairment (e.g., the water-filled tap), back to the first (e.g., the amplifier output), and then some of that energy continues downstream; it is an attenuated version of the first signal but delayed. This causes an impact on the signal that appears as an amplitude ripple in the spectrum data, such as at a cable modem connected to the cable. The standing wave will appear as a periodic amplitude change along the length of the cable (Figure 1). The graphic in the figure shows three sections of coaxial cable with the middle section having impedance mismatches on both sides. The area within the middle section is where the signals are interfering constructively and destructively between two impedance mismatches, sometimes called the impedance or echo cavity. The impedance cavity has directional properties, with the input coming from the direction of the transmitter and the output towards the receiver. At the output of the impedance cavity, one or more additional copies of the signal are present, with additional delay and attenuation. This is illustrated by the large arrow indicating the flow of the incident signal through the cable and the second smaller arrow trailing behind it. This second signal in the figure is intended to represent a delayed copy of the incident signal, created by the impedance cavity.

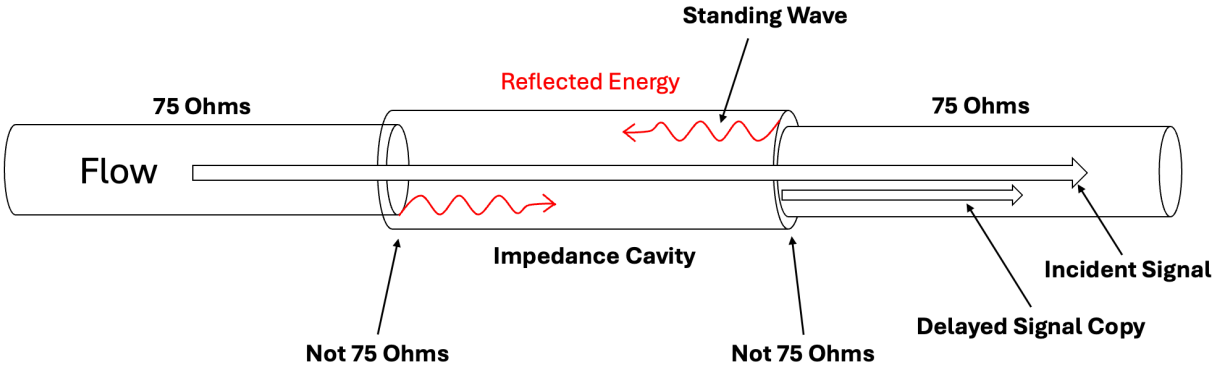

Figure 1 – Impedance Mismatches, Return Loss, Reflections and Standing Waves

In the Data-Over-Cable Service Interface Specifications (DOCSIS®) 3.1 specifications, both OFDM and OFDMA were standardized, including an optional pre-distortion for upstream OFDMA carriers. For both modulation types, management information base (MIB) objects were specified to reveal the frequency domain complex coefficients associated with each of the potentially thousands of active subcarriers. A MIB object request is sent to the CM, and the CM performs a Trivial File Transfer Protocol (TFTP) transfer of a file containing the requested in-phase (I) and quadrature (Q) coefficients. Note that the upstream coefficients returned are for the corrections to mitigate non-flat frequency response due to impairments, not for the impairments themselves; the coefficients describe the CM pre-equalizer, which has a frequency response which is approximately the inverse of the plant frequency response. For the downstream OFDM channels, the CM can report channel estimation coefficients, also as complex coefficients. Those channel estimation coefficients approximate the network frequency response, and therefore can also indicate any impairments.

For both upstream and downstream SC-QAM signals, the returned complex coefficients are in the time domain. Conversely, in multi-carrier systems such as DOCSIS OFDM and OFDMA channels, the returned coefficients are in the frequency domain. The fast Fourier transform (FFT) and inverse fast Fourier transform (IFFT) can be used to convert between time and frequency domains.

Figure 2 from Alberto Campos shows block diagrams of the transmitter and receiver processes where the pre-equalization (at the upstream transmitter) and channel estimates (at the downstream receiver) are used. The transmitter process is shown in the upper portion of the diagram, with the pre-equalization frequency points (in red) being implemented just after the frequency points are generated by the symbol mapper and before the IFFT process, occurring in the frequency domain. The lower part of the figure shows the receiver process with the downstream equalization occurring after the FFT and before the symbol mapping (in red), also in the frequency domain.

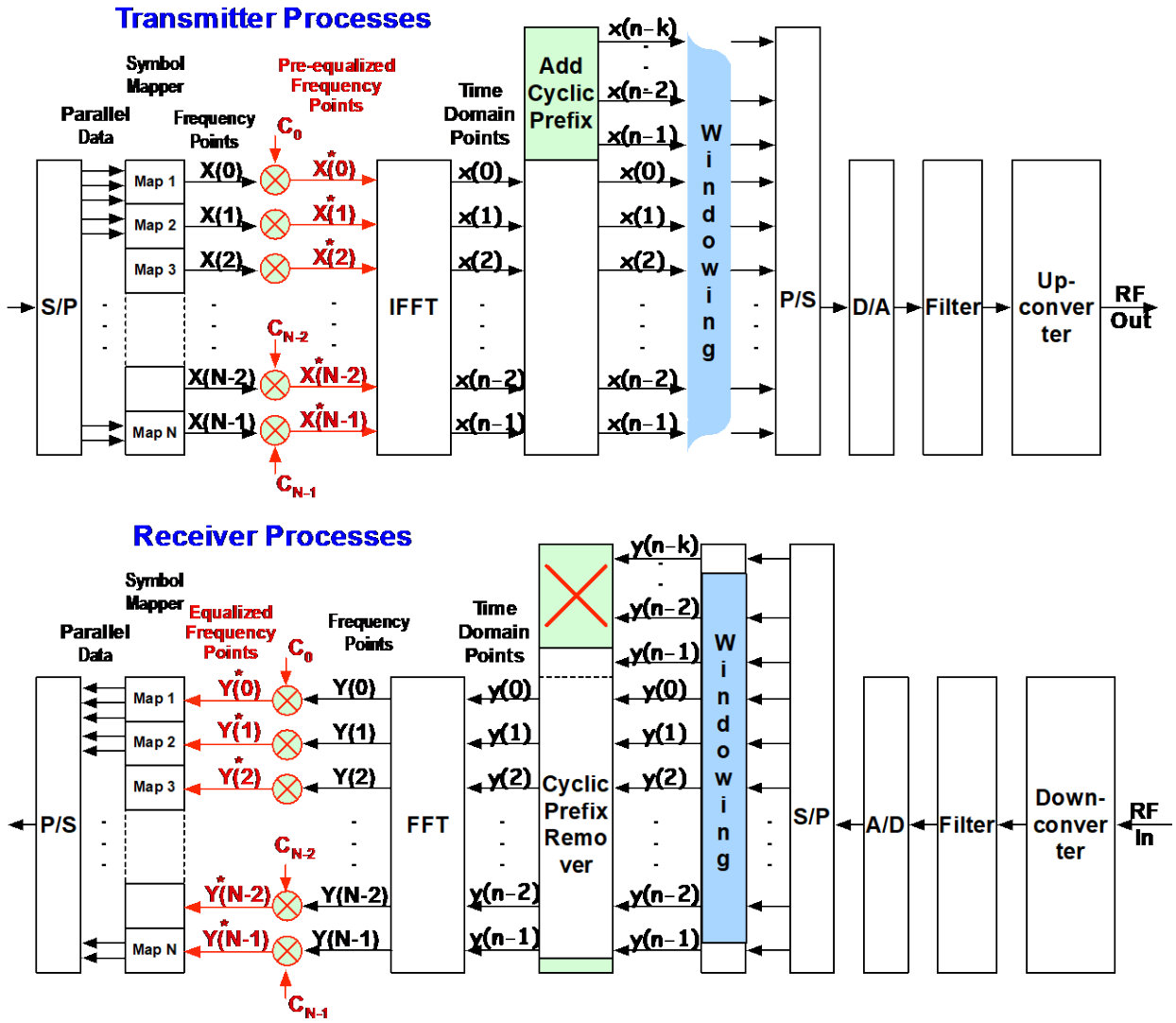

Figure 2 – DOCSIS Transmistter and Receiver Block Diagrams; Courtesy of Alberto Campos, CableLabs

3. PNM Data

In DOCSIS 3.0 systems, pre-equalization coefficient and full-band capture (FBC) data are obtained using Simple Network Management Protocol (SNMP) to request information from CMs and converged cable access platforms (CCAPs). The requested information is described in [2], and the SNMP MIB objects are defined in [3].

DOCSIS 3.1 technology introduced new requirements for CMs and cable modem termination systems (CMTSs) related to the collection and reporting of PNM data (see [4], Section 9, "Proactive Network Maintenance"). DOCSIS 3.1 also introduced a new bulk-data transfer mechanism that uses TFTP to upload PNM data to a destination TFTP server. Configuration of the PNM test execution parameters, file storage, and TFTP destination uses SNMP as defined in [5] and [6].

Figure 3 shows the steps and communication paths involved in collecting PNM data from a CM or CCAP device. This flow chart was originally published in the PNM Best Practices document [2]. The figure shows a sequence diagram between three processes: starting on the left is the PNM server, then the TFTP server, and the CM/CCAP on the right. There are seven sequential operations:

1. The PNM server will use SNMP to SET the bulk file control parameters on the CM/CCAP.
2. The PNM server will use SNMP to SET the test operation on the CM/CCAP.
3. The PNM server will use SNMP to GET the test operation status from the CM/CCAP.
4. Optionally: the CM/CCAP may initiate the TFTP file transfer if requested (to TFTP server).
5. Optionally: the CM/CCAP may transfer the PNM file containing the measurements.
6. The PNM server will use SNMP to GET the test operation results from the CM/CCAP.
7. The PNM server will use TFTP to retrieve the PNM file from the TFTP server.

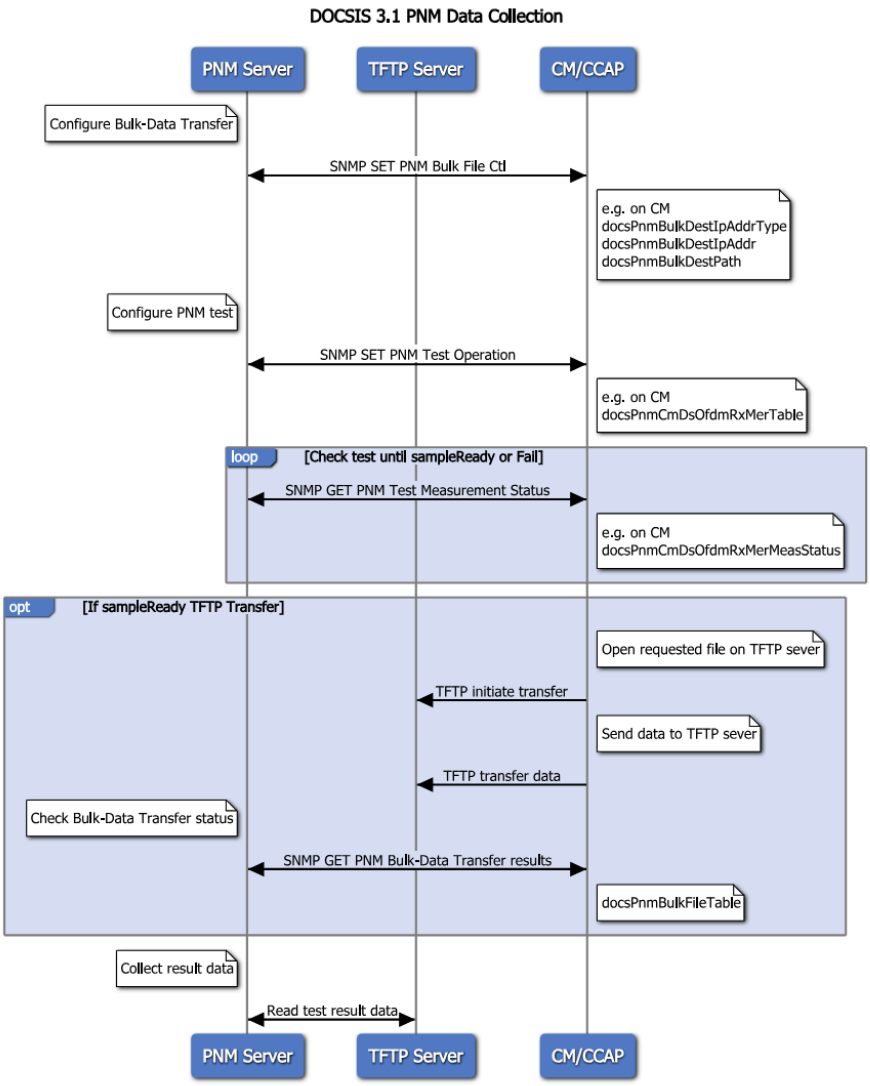

Figure 3 – Data Collection Sequence Diagram, From [2]

When complete, a PNM test result file is produced and uploaded, that a PNM application can decode and analyze. Unless explicitly changed, the default PNM test result file name contains the PNM test name, a unique identifier like the CM MAC address, and a timestamp. The PNM test file is a binary data file containing a header and a data section as defined in [5] and [6].

3.1. Specifications

The DOCSIS PNM Best Practices [2] document describes many capabilities. While the PNM Best Practices [2] document focuses on SC-QAM equalization techniques, this paper focuses on the improved capabilities associated with OFDM and OFDMA. Further details are provided in the DOCSIS 3.1 specifications [5], which applies to DOCSIS 4.0 technology as well.

In sections D 2.6 (channel estimation coefficients) and D 2.13 (pre-equalization) of [5], there are explanations of how these tests work and are executed, including the MIB definitions, and how to read the

tables that are delivered. The specification also provides definitions for the results delivered by the tests; the object attributes are defined and listed in tables to make it easier to decode the files that provide the test results. For decoding details and examples please refer to Appendix A.

3.2. Processing

Much work on coefficient processing has been done by Tom Williams et al, described in his 2021 paper [1], and by others including Roger Fish and Tom Kolze. Tom Williams presented the processing steps for correcting raw phase data (directly from the CM and CMTS) to remove the arbitrary addition of linear phase delay from the coefficients. In addition to a thorough explanation in his paper, Tom Williams and co-authors generously included C++ code examples to facilitate the implementation.

While this processing is helpful and explanatory, it isn't entirely necessary to make use of the information contained in the coefficients. Simplified alternative methods are described later in sections 3.2.1 and 3.2.2. However, by correcting the phase of the complex values, more powerful digital signal processing (DSP) techniques can be used to analyze the data. Section 4 of this paper covers different analysis methods and section 4.5 covers some of the more advanced techniques using DSP.

Preprocessing of the frequency response coefficients corrects two major aspects: linear phase rotation over frequency in frequency domain and impulse response at time equal 0 in time domain is real (phase is 0º). This method involves two main steps:

Coarse Delay Removal: This step is performed in the frequency domain. Average phase rotation over frequency is calculated and removed. This step affects only the phase component in the frequency domain. Performing coarse delay removal effectively brings the main bin of the impulse response to time equal 0 in the time domain.

Fine Phase Adjustment: This step is performed in the time domain. The phase of the impulse response shifted such a way that the main bin of the impulse response is real (phase is 0º at time equal 0). Results of this adjustment needs to be transformed back to the frequency domain to obtain the corrected channel estimate.

With this calibration, the remaining signal more accurately reflects the plant condition in a uniform way, allowing for precise data processing and analysis and comparison across multiple modems.

3.2.1. Frequency Domain Analysis Without Processing

It is possible and sometimes useful to use the equalizer and channel estimate coefficients without processing. Tom Williams's routine for removing the linear phase delay allows samples to be directly compared on a complex plane because it normalizes their phase components. However, the linear phase delay in the time domain is uniform and thus shifts all the frequency components by the same amount without changing the magnitude of those components. Because the amplitude vs. frequency response doesn't require phase correction, the complex coefficients may be used directly without processing to evaluate the approximate frequency response of the channel. This is useful for doing frequency domain analysis of the equalizer responses, such as peak-to-valley, ripple detection and tilt measurements. By eliminating the processing step, some computational time and complexity may be saved. While this might seem trivial, large cable systems may have tens of millions of samples to process so even small improvements can provide compounding savings to the implementer. Figure 4 and Figure 5 show a comparison of corrected and uncorrected values in the frequency domain. Notice that the amplitudes are identical, with and without correcting the linear phase delay.

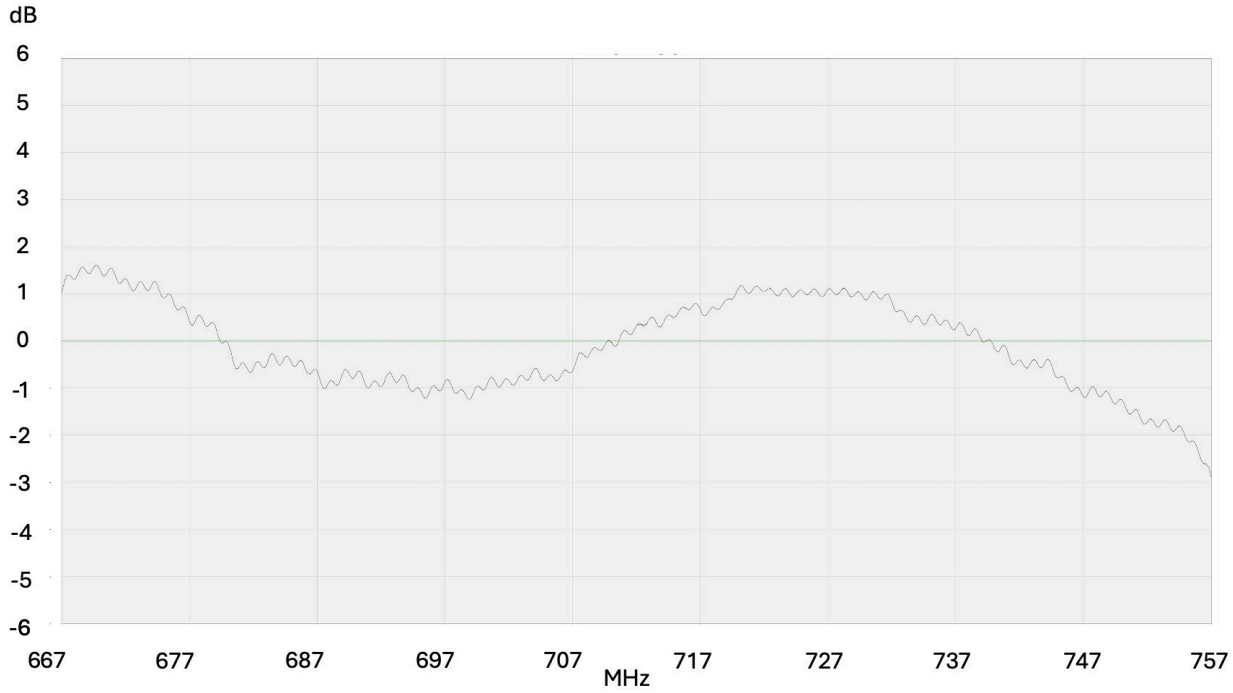

Figure 4 – Corrected Amplitude vs. Frequency Response

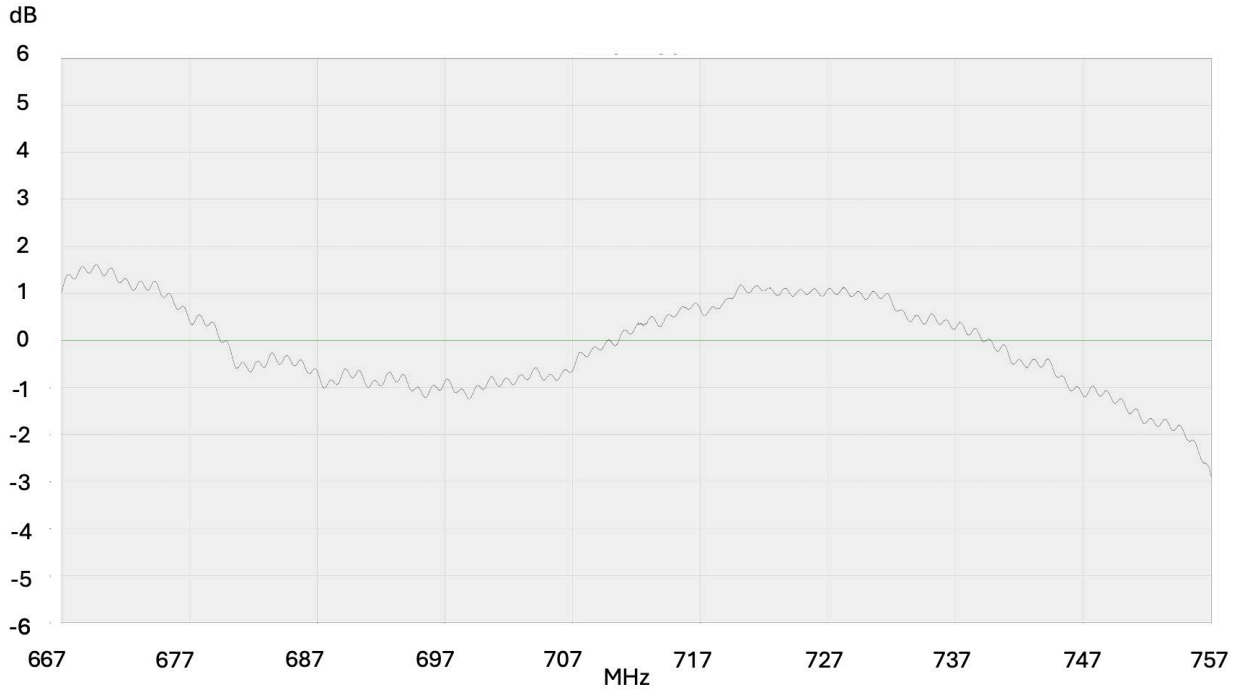

Figure 5 – Uncorrected Amplitude vs. Frequency Response

3.2.2. Time Domain Analysis Without Processing

It is also possible to use the raw time domain coefficients after inverse Fourier transformation from the frequency domain. There may be an arbitrary linear phase delay in the time domain, which shifts the main tap position to the right some amount of time (bins). The impulse response components (time intervals) in the time domain remain consistently spaced from the main tap position, regardless of the main tap position. For example, Figure 6 shows an impulse response with an echo that is spaced at 78 bins from the main tap position of 0. The same response using the uncorrected coefficients that contain the linear phase delay can be seen in Figure 7. Notice the main tap location is shifted by 55 bin positions to the right, but the echo component maintains its relative spacing of 78 bins, which is position 133.

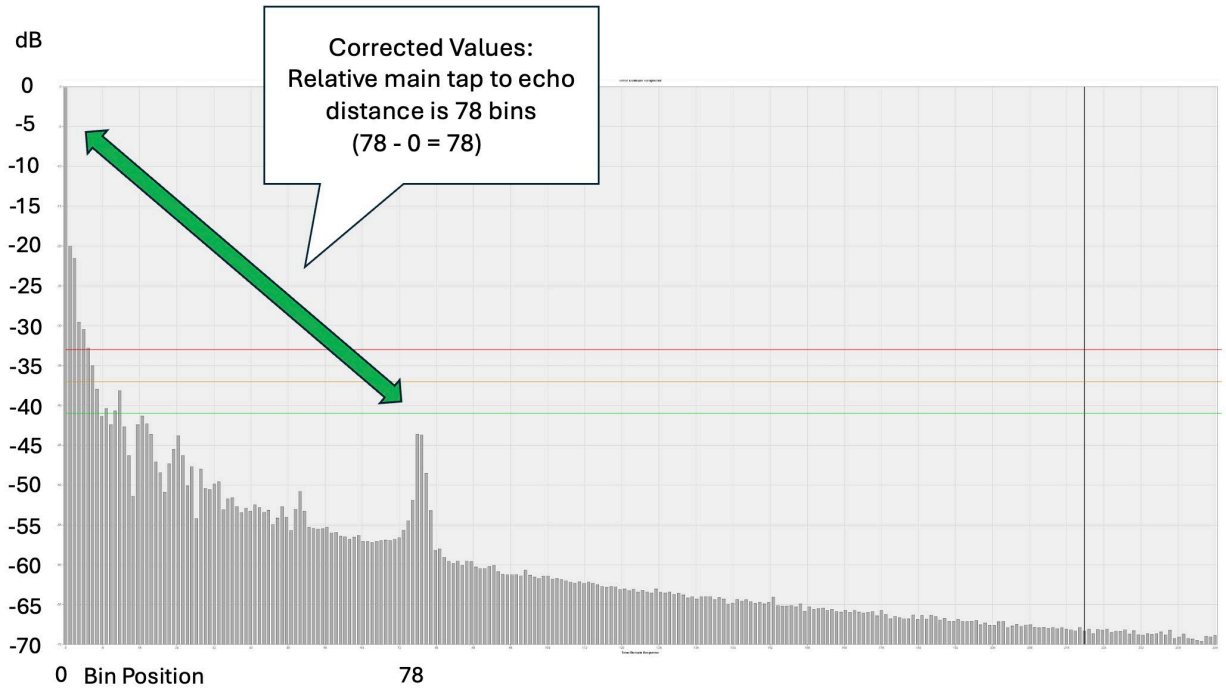

Figure 6 – Corrected Time Domain Impulse Echo Relative Distance

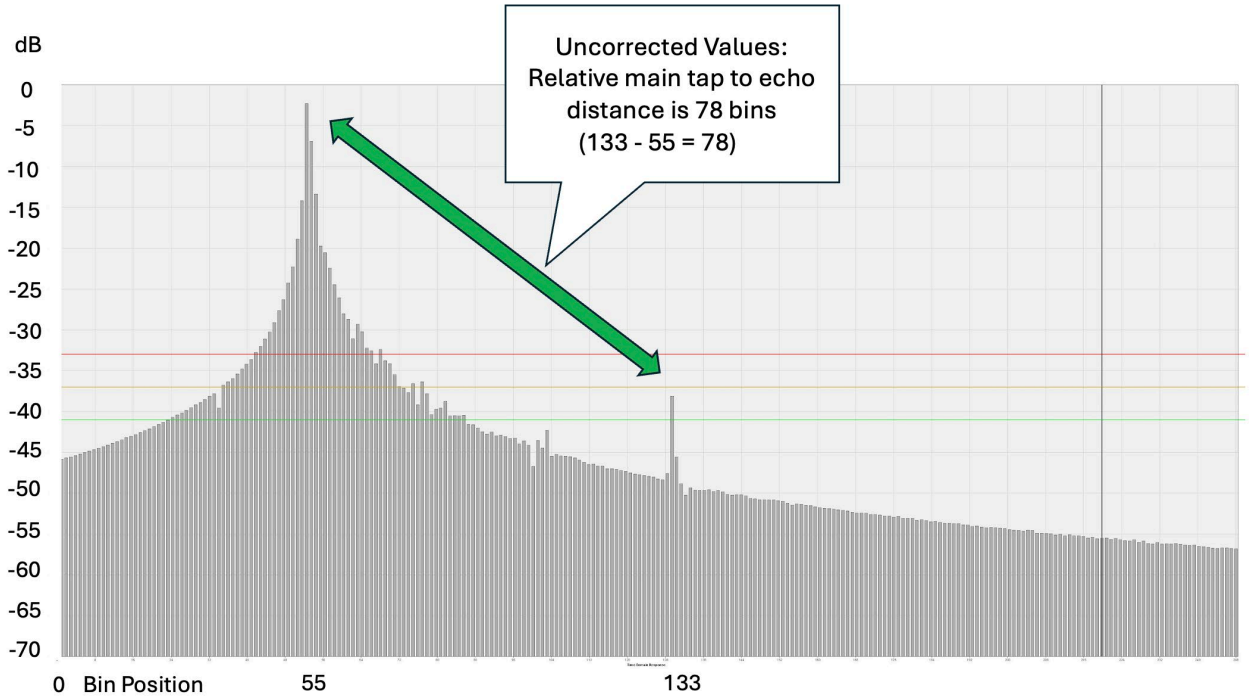

Figure 7 – Uncorrected Time Domain Impulse Echo Relative Distance

4. Analysis

4.1. Outlier Data

Occasionally, while evaluating the upstream OFDMA adaptive pre-equalizer coefficients and downstream OFDM channel estimates from live plant data, some anomalous examples were observed. These examples contained larger-than-usual amounts of energy in the time domain that were not explainable by expected or rational amounts of reflected energy caused by degraded return loss.

4.1.1. Channel Noise and Ingress

When significant noise-like interference was present within the downstream OFDM channel, amplitude variation was observed in the frequency domain components, seen circled in red in Figure 8.

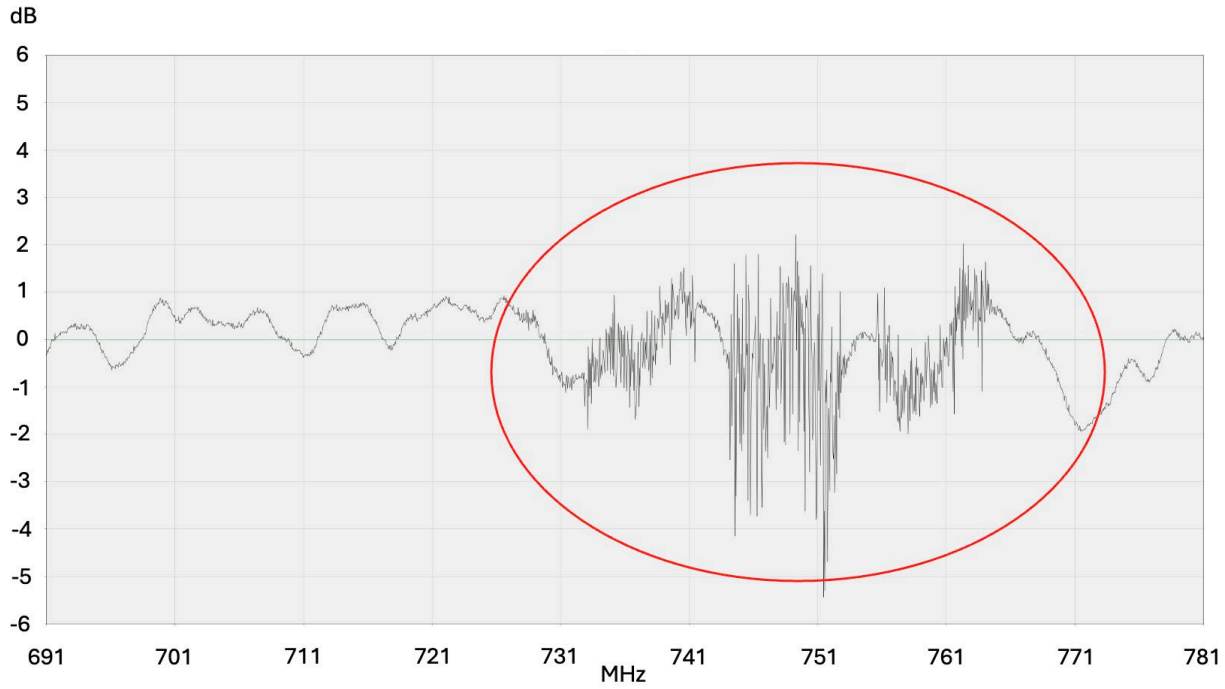

Figure 8 – LTE Ingress Interference Within a Downstream OFDM Channel, Frequency Domain

After the inverse Fourier transformation, these additional frequency components result in dispersion over a longer period. The interference within the channel becomes spurious energy that is spread over time, making it more difficult to analyze when looking for echoes in time domain (Figure 9). Because it is limited to a certain frequency band, we can be confident that the cause is ingress.

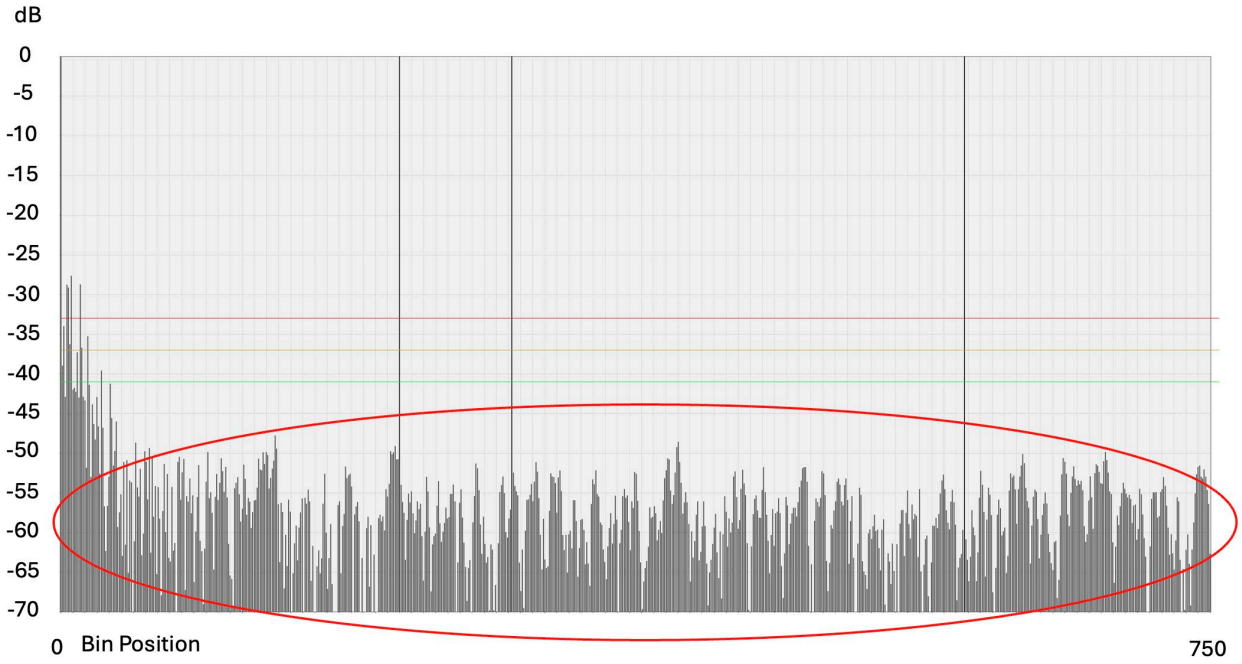

Figure 9 – LTE Ingress Interference Within a Downstream OFDM Channel, Time Domain

The ingress can be confirmed using a PNM FBC spectrum display, showing unwanted signals within and outside of the OFDM occupied spectrum, appearing as interference over a range of frequencies. Figure 10 shows the uneven OFDM channel spectrum circled in red. Notice additional ingress in the FM band (from 88 MHz to 108 MHz), and in between 800 MHz and 900 MHz.

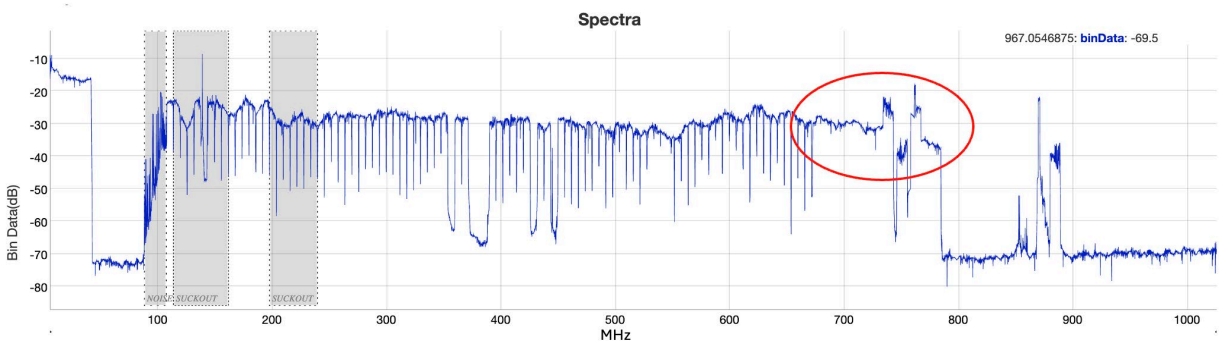

Figure 10 – Ingress Interference Within a Downstream OFDM Channel, FBC Frequency Spectrum

4.1.2. Channel Tilt

There are examples where significant tilt was present within the channel, indicating a strong drop off in signal strength as the frequencies increase (Figure 11).

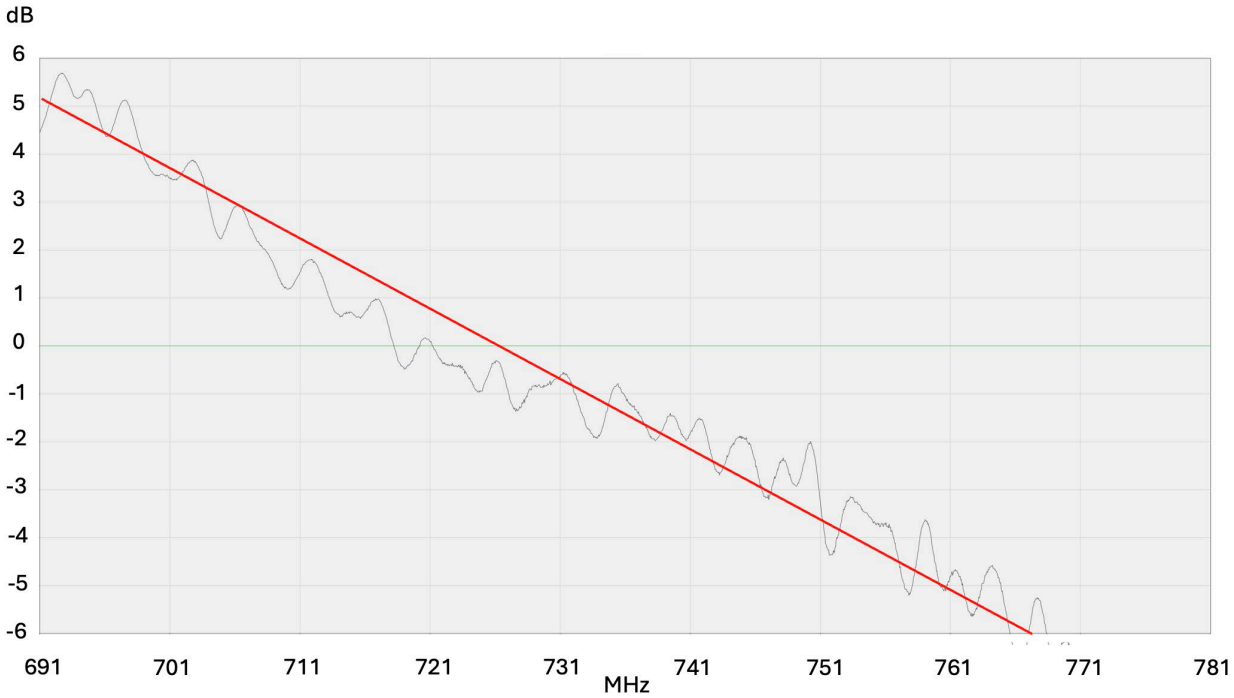

Figure 11 – 14 dB of Tilt Within Downstream OFDM Channel, Frequency Domain

When applying the inverse Fourier transformation, the result is a right-sided exponential decay in time (Figure 12) indicated by the red line, sloping downward. This is analogous to an “input” impulse signal spreading out and decaying over time, analogous to a lowpass filter time domain response. The frequency domain down tilt represents the signal losing strength at higher frequencies.

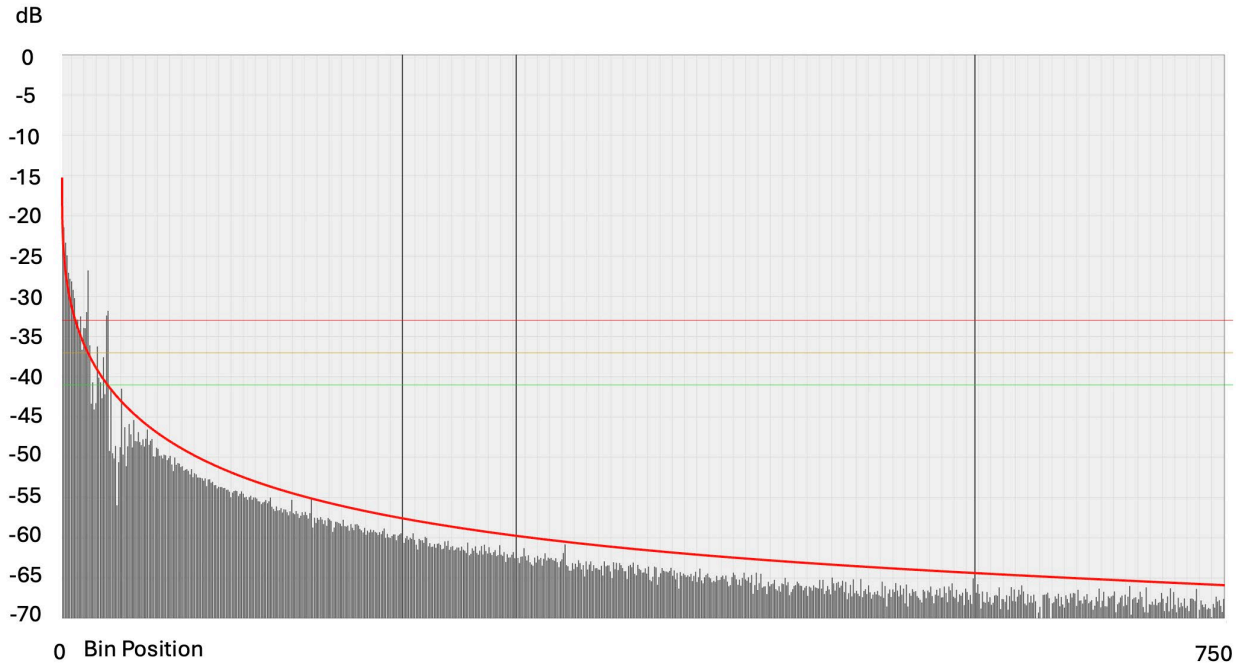

Figure 12 – 14 dB of Tilt Within Downstream OFDM Channel, Time Domain

Again, confirming the power spectrum using PNM FBC, the tilt within the OFDM spectrum can be observed in Figure 13, circled in red. Notice approximately 14 dB of tilt within the 96 MHz occupied bandwidth of the OFDM spectrum, compared to the approximately 32 dB of tilt across the entire occupied spectrum.

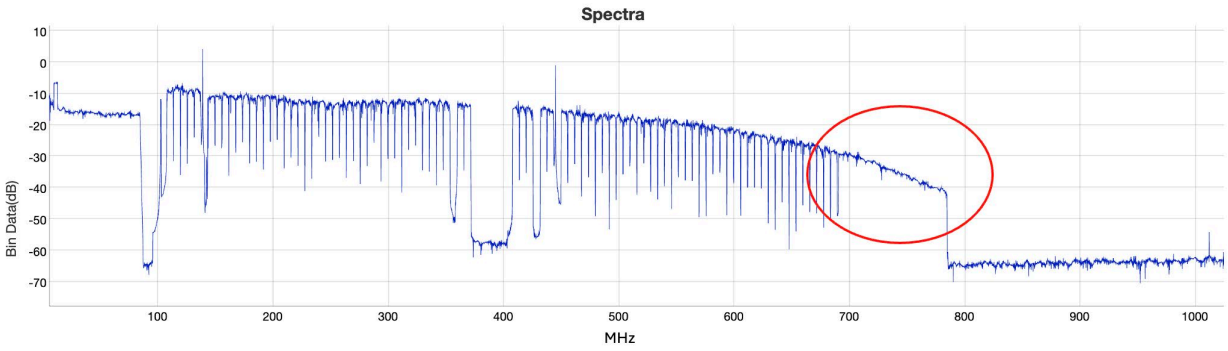

Figure 13 – 14 dB of Tilt Within Downstream OFDM Channel, Time Domain

4.2. Impulse Response

One common method for echo detection is locating peaks within the time domain impulse response. The magnitude of the peak can be calculated, and the time delay converted to distance. Sections 4.3 and 4.4 describe the magnitude and time-to-distance calculations. Together, these values can provide an approximate measurement of impedance cavities caused by impedance mismatches within the transmission lines such as coaxial cables and passive components.

4.3. Magnitude

The impulse response magnitude is calculated in the time domain as the square root of the vector sum of the real and imaginary components. It was shown in section 3.2.1 that the magnitude in the frequency domain is the same, regardless of the linear phase delay being present or removed. However, the magnitude of the impulse response bins is dependent on the phase angles which can be variable, given the arbitrary nature of the linear delay. The two charts in Figure 14 illustrate the issue, with the corrected time domain bins in the chart on the left and the raw bins on the right. Notice the reflection on the left has energy quantized between bins 78 and 79, while the chart on the right has the energy concentrated 79 bins away from the main tap position. This is because the correction routine removes a linear phase delay and rotates the main tap phase to 0 degrees. This process results in some potential phase change in all the subsequent time domain components. In our example, the phasor ends up in a position closer to the middle of bins 78 and 79 (0 or 180 degrees) rather than something closer to 90 or 270 degrees of bin 79.

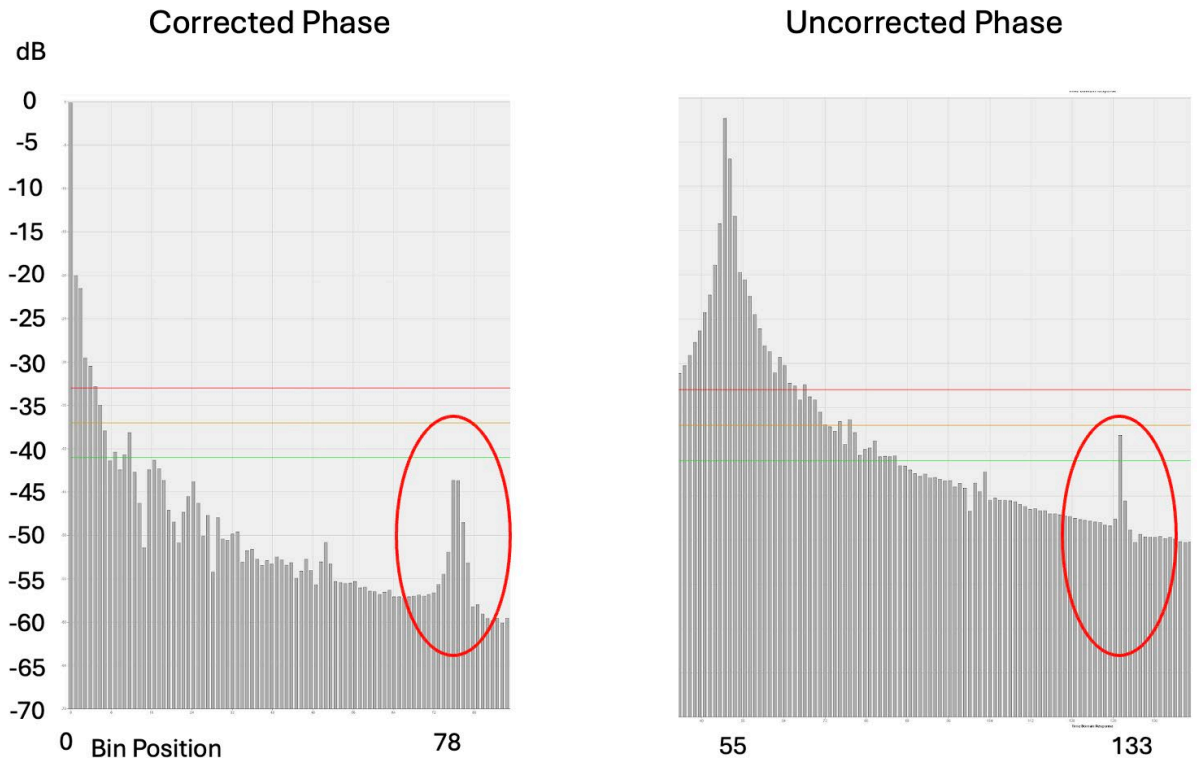

Figure 14 – Corrected vs. Uncorrected Impulse Response Quantization

4.4. Time and Distance

In DOCSIS systems, the downstream sampling rate is 204.8 MHz, and the upstream sampling rate is 102.4 MHz. The FFT/IFFT size depends on the sampling rate and subcarrier spacing. For downstream OFDM channels, the FFT size is 8192 for 25 kHz subcarrier spacing and 4096 for 50 kHz subcarrier spacing. Respectively for upstream OFDMA channels FFT size is 4096 for 25 kHz and 2048 for 50 kHz. This means that, in the downstream after performing the IFFT on the frequency response, the time domain will span 20 µs or 40 µs (for 50 kHz and 25 kHz subcarrier spacing respectively), with a time granularity of 1/204.8 MHz or 4.8828 ns.

So, in theory, after you take the inverse Fourier transform to obtain the time domain response, the difference in bins between the main tap and the reflection is 4.8828 ns per bin. This is the round-trip delay of the signal traversing the reflection cavity. Then, multiply the previous result by the propagation factor of the cable and the speed of light to obtain the round-trip time. Finally, divide the round-trip time by two for the impedance cavity length.

$$L = \frac{c \cdot VoP \cdot \frac{1}{R_s}}{2} \cdot t = c \cdot VoP \cdot T_r \cdot t = L_r \cdot t$$

$$T_r = \frac{1}{2 \cdot R_s}, \qquad L_r = c \cdot VoP \cdot T_r$$

- L – estimated length of the resonant cavity (not round-trip[1]), ft
- c – the speed of light in a vacuum in feet per second (983,571,088 ft/s)
- R_s – sampling rate, Hz. 204.8 MHz for ODFM and 102.4 MHz for OFDMA channels
- T_r – theoretical time resolution for each bin (not round-trip), s
- L_r – theoretical cable distance resolution for each bin (not round-trip), ft
- VoP – velocity of propagation (VoP). 85% (or 0.85 c) typical of series 11 cable
- t – number of bins from main tap

The following values represent the theoretical time resolutions for each bin:

- 204.8 MHz downstream sample rate of OFDM is 2.4414 ns (or 4.8828 ns round-trip)
- 102.4 MHz upstream sample rate of OFDMA is 4.8828 ns (or 9.7656 ns round-trip)

In practical application, additional factors must be considered. The number of active subcarriers in the OFDM/OFDMA channel is not equal to the FFT size and depends on the configured OFDM/OFDMA channel width. Because of this, when taking the inverse Fourier transform of channel, the estimated time resolution changes with the ratio of the number of active subcarriers and the FFT size.

$$T'_r = \frac{1}{2 \cdot R_s} \cdot K$$

$$K = \frac{FFT_{size}}{N_{active}} = \frac{R_s}{Bw_{channel}}$$

- T'_r – adjusted time resolution for each bin (**not** round-trip), s
- K – FFT correction factor

[1] The signal travels through a resonant cavity at least two extra times (as described in section 2).

- FFT_{size} – FFT size used for the channel, as described above
- N_{active} – number of active subcarriers
- R_s – sampling rate, Hz
- $Bw_{channel}$ – bandwidth occupied by the channel, Hz

This correction coefficient (FFT_{size}/N_{active}) is then applied to the theoretical distance to obtain real distance of the resonant cavity:

$$L' = L_r \cdot t \cdot K = L \cdot K$$

4.4.1. OFDM Downstream Channel Estimate Coefficients

As established earlier, theoretical time resolution for the OFDM channel is 2.4414 ns for each channel estimate bin. For series 6 cable, this translates to about 2.04 ft for each bin (assuming velocity factor of 0.85):

$$L_r = \frac{983{,}571{,}088\ (ft/s) \cdot 0.85}{2 \cdot 204.8\ (MHz)} \approx 2.0411\ ft$$

This value must be corrected based on the number of active subcarriers. For example: for a 192 MHz wide OFDM channel with 190 MHz active bandwidth there will be 3800 active subcarriers for 4096 FFT (50 kHz spacing) and 7600 active subcarriers for 8192 FFT (25 kHz spacing). Thus, the FFT correction factor will be the same for either FFT size or equal to:

$$K = \frac{8192}{7600} = \frac{4096}{3800} = \frac{204.8\ MHz}{190\ MHz} \approx 1.0779$$

The actual channel estimate time domain bin cable length resolution for this configuration will be:

$$L = 2.0411\ ft \cdot 1.0799 \approx 2.2\ ft$$

This value would change slightly for cables having a different velocity of propagation.

4.4.2. OFDMA Upstream Pre-Equalization Coefficients

The theoretical time resolution for each OFDMA channel is 4.8828 ns for each pre-equalization time domain bin. This translates to about 4.08 ft over series 6 cable (assuming velocity factor 0.85):

$$L_r = \frac{983{,}571{,}088\ \left(\frac{ft}{s}\right) \cdot 0.85}{2 \cdot 102.4\ (MHz)} \approx 4.0822\ ft$$

Based on the number of active subcarriers this value must be corrected. For example: for 24 MHz wide OFDMA channel with 22 MHz active bandwidth there will be 440 active subcarriers for 2048 FFT (50 kHz spacing) and 880 active subcarriers for 4096 FFT (25 kHz spacing). Thus, the FFT correction factor will be the same for either FFT size equal to:

$$K = \frac{4096}{880} = \frac{2048}{440} = \frac{102.4\ MHz}{22\ MHz} \approx 4.6545$$

The actual pre-equalization time domain bin cable resolution for this configuration will be

$$L = 4.0822\ ft \cdot 4.6545 \approx 19.0\ ft$$

This value might change slightly for cables having a different velocity of propagation.

4.5. Frequency Response Matching and Other DSP Techniques

One of the primary benefits of using Tom Williams's phase correction routine is that it removes the arbitrary linear delay that is added to the measurements, resulting in uniform phase values across a population of measurements. Without this correction, a random delay may be added to samples, making them unusable for complex analysis using common DSP techniques such as complex products, quotients and other operations that include comparison of phase components of the signal. Figure 15 shows an example of complex division for matching frequency response signatures using SC-QAM coefficients.

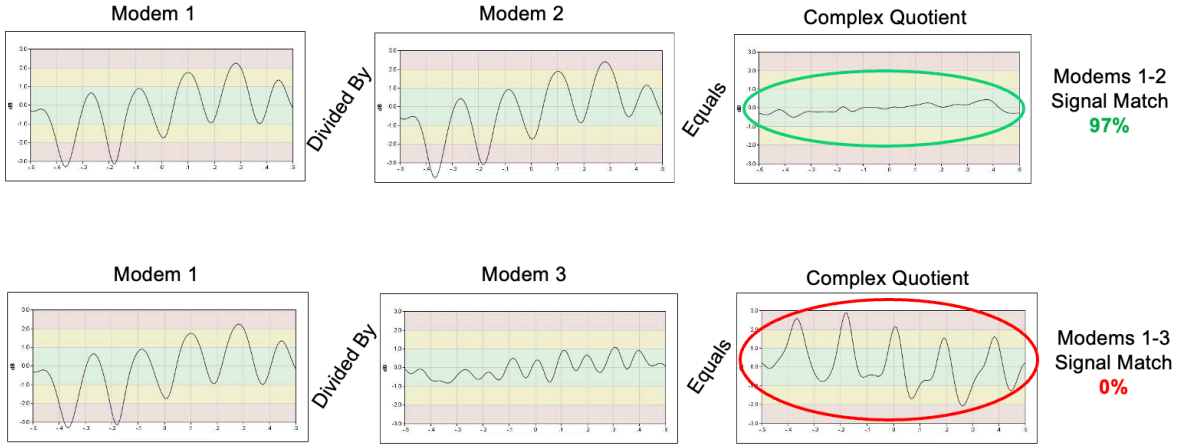

Figure 15 – Example of Complex Division for Signature Matching

Figure 16 shows the results of a complex division operation comparing two identical OFDM channel estimates that have the phase components corrected. Note that the complex division results in an exact match in the quotient. The frequency vs. amplitude of the quotient is a perfectly flat response. Likewise, the time domain of the quotient is a single main tap value with no residual components.

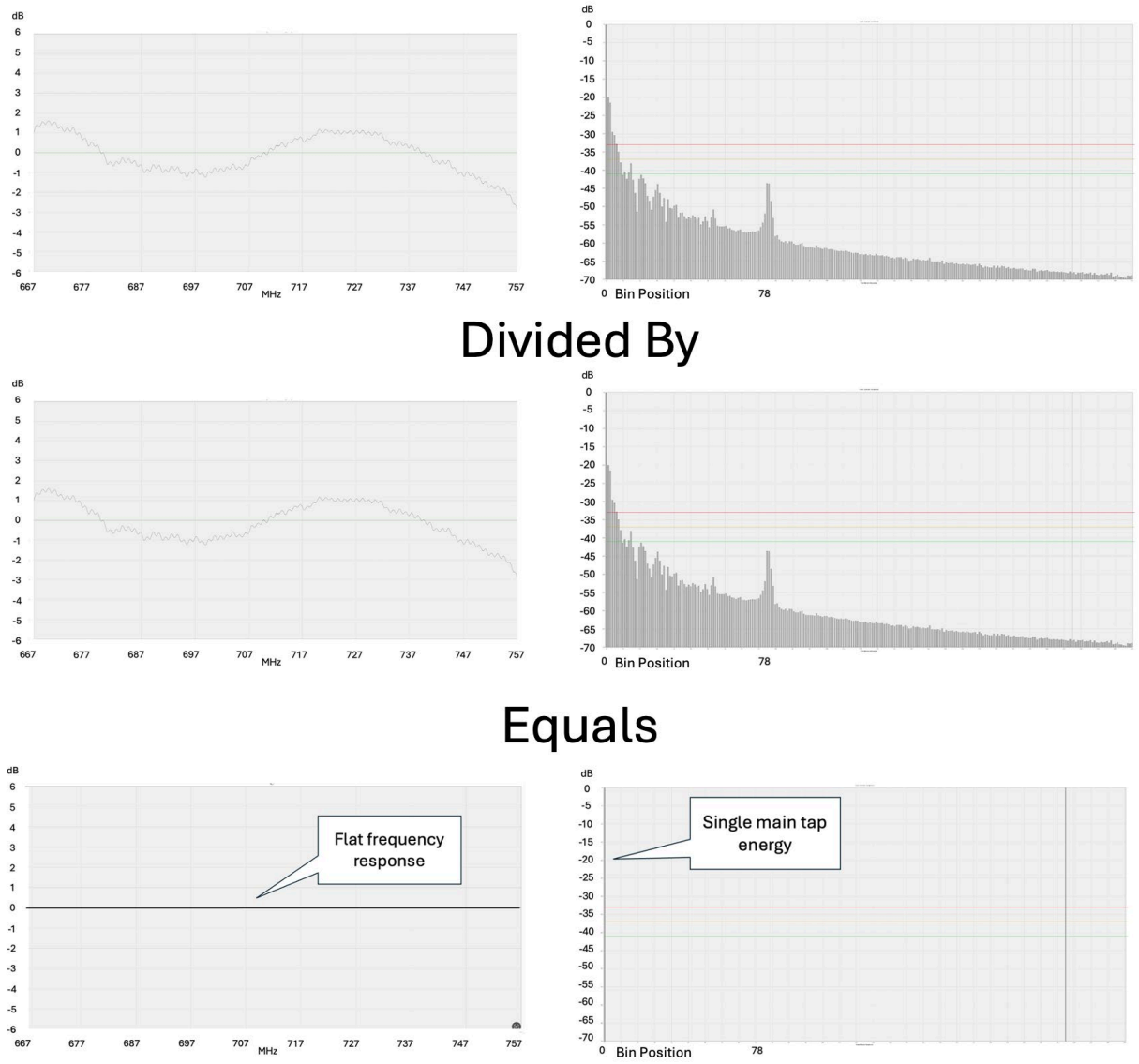

Figure 16 – Complex Division of Two Phase Corrected OFDM Samples

Figure 17 shows the results of complex division of OFDM channel estimates when the phase components are not the same (uncorrected). You can see that the frequency responses are the same but the main tap locations are different in the time domain. The result of the complex division in this example is a power offset in the frequency domain and an irrational impulse response. This is the one of the primary motivations for removing the linear phase delay. Still, if one sees a result such as in Figure 17, it is a clue to use a better method to remove the linear phase delay.

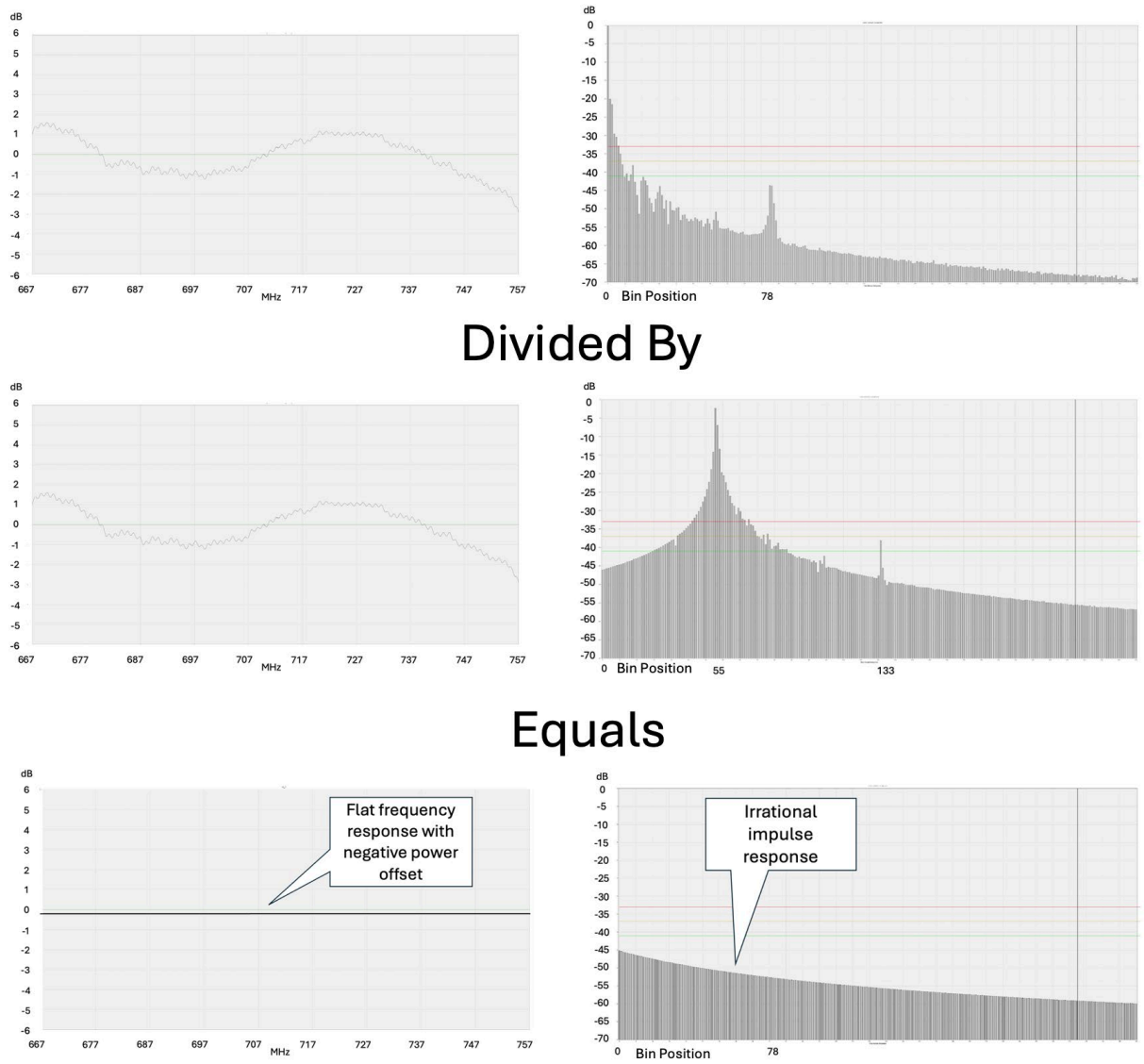

Figure 17 – Complex Division with Mismatched Phase Components

5. Benefits

Having reviewed the fundamentals of obtaining, decoding, and processing the OFDM and OFDMA PNM measurements, this section discusses the potential benefits of the work. For a broader perspective about the benefits of PNM tools and techniques, see the 2016 SCTE paper, "A Comprehensive Case Study of Proactive Network Maintenance" [7] by Wolcott, Heslip et al.

5.1. Increased Resolution and Accuracy

Going back to the PNM roots in DOCSIS 2.0 and 3.0 PNM, there are limits to the time and frequency resolution of the SC-QAM measurements. When comparing the upstream SC-QAM distances with those of OFDMA, section 5.11 shows the distance calculations being improved from approximately 85 feet per tap, to eight feet. This is approximately 10 times better upstream distance resolution. Note that the early

PNM implementations generalized the length to 85 feet-per-tap to make it easier for technicians to do the calculations. The real length is around 83 feet with a VoP of 87% for typical hard line coaxial cable.

5.1.1. Upstream Pre-Equalization Coefficients

Tom Kolze describes the SC-QAM equalizer calculations in the following material adapted from "Pre-Equalization Based Upstream Frequency Response Measurements" [8]. Tom states, "In the case of single carrier quadrature amplitude modulation (SC-QAM) signals, it can be shown (T. Kolze) that the derived equalizer response is a superposition of some number N different filter responses (that is, the number of pre-equalizer taps). Each of the N filters' center frequency is spaced 1/NT Hz from its adjacent filter (in frequency, where N is the previously mentioned number of pre-equalizer taps and T is the symbol period in seconds). Each filter has an equivalent noise bandwidth (ENBW) of 1/NT Hz. Thus, the equalizer response comprises a sum of frequency responses, where each of the N frequency responses has a resolution bandwidth (RBW) of 1/NT Hz, providing a very similar, but not exactly the same response. as with a conventional sweeping spectrum analyzer."

- N = 24 pre-equalizer taps
- T = 1/ (5,120,000 symbols per second) = 1.95E-7 second
- Solving the equation above gives 1/(24*1.95E-7) = 213.33 kHz

Figure 18 shows a graphic representation of four different cable faults, each having progressively longer fault distances. Starting with the graph on the left, a 1T reflection indicates a maximum length of 85 feet. Then 2T with 85 feet to 170 feet, 3T with 170 feet to 255 feet, and finally, 4T with 255 feet to 340 feet distance. Notice that each time bin, or T, is measured in relative distance from the main tap position (8). The first chart shows large bars sticking up at position 9, so that is 9-8=1, hence a 1T reflection. These reflections have a distance resolution of approximately 85 feet. Further details about upstream pre-equalization coefficients can be found in [9].

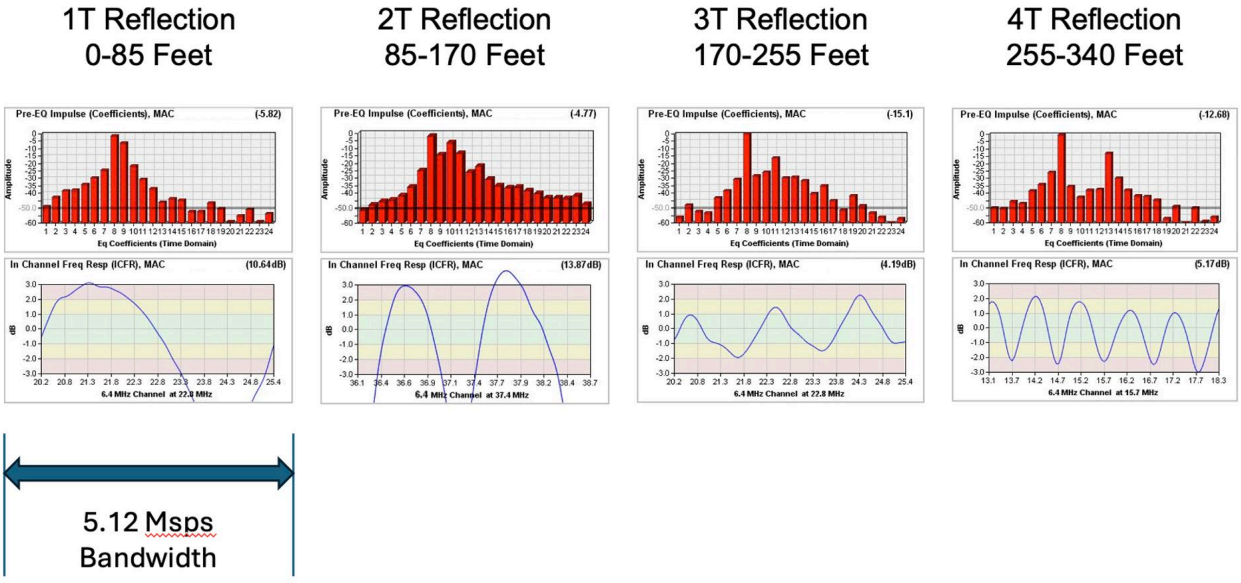

Figure 18 – SC-QAM Impuse Response Distance Example (6.4 MHz Wide Channels)

When considering the coefficients of OFDMA, the resolution is greatly improved. The frequency resolution of the OFDMA coefficients is determined by a sample rate. Figure 19 shows an example of a damaged coaxial cable at 875 ft distance from the amplifier. The upstream pre-equalizer from one of the

SC-QAM channels centered at 36.5 MHZ has a large echo at tap position 18, which is 10T in distance from the main tap at position 8. With 85 ft per T distance resolution, the SC-QAM impulse response shows an 850 ft length of the impedance cavity.

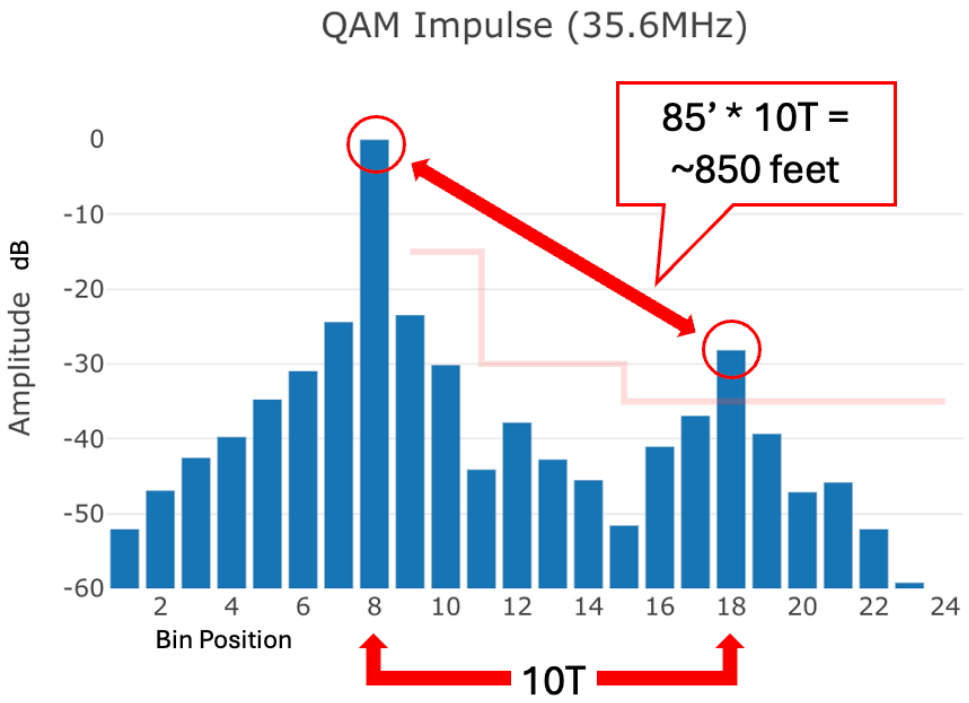

Figure 19 – 24-Tap SC-QAM Pre-Equalizer Fault Distance Example

Figure 20 is a chart showing the same plant fault using the upstream coefficients obtained from the OFDMA channel, which has 51 MHz of contiguous active subcarriers, centered at 58 MHz and with 50 kHz sub-carrier spacing. In this example, the impulse response echo has 107 bins separating it from the main tap position of 0. The math shows that the impedance cavity is calculated at 877 feet, which is significantly closer to 875 than the previous estimate of 850.

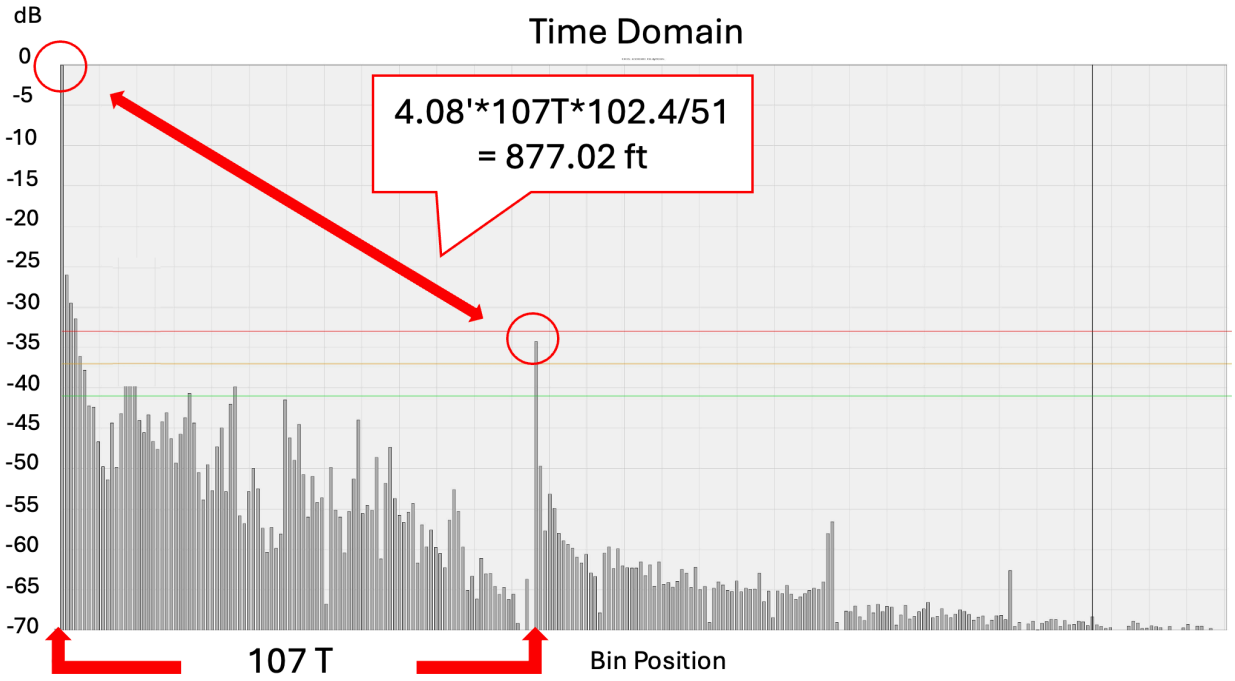

Figure 20 – OFDMA Pre-Equalizer Time Domain Fault Distance Example

5.1.2. Downstream Channel Estimates

As for the downstream OFDM channel estimates, there is no pre-existing PNM capability that is directly analogous. The downstream SC-QAM equalization coefficients were eventually defined to have a finite impulse response (FIR) structure, but prior implementations are not consistent across the many CM products and have not been used. The two features of PNM most used for downstream analysis are FBC and RxMER per subcarrier. Both capabilities are useful tools for different types of detection and analysis, but the channel estimate fills some of the gaps within their usefulness.

FBC is excellent for evaluating large spans within the power spectrum but generally requires averaging to produce useful measurements. As a result, small amplitude changes are difficult and sometimes impossible to detect in a practical manner. RxMER per subcarrier is probably the most used feature of PNM, but the measurement is taken after the subcarrier equalization occurs and lacks I and Q information, which is useful for more precise distance calculations.

5.2. Greater Sensitivity

There are several factors that contribute to improved sensitivity in DOCSIS 3.1 and 4.0 PNM measurements. A number of those are outside the scope of this paper so here we focus on the sensitivity improvements associated with using a higher-order FFT and increased sample rate.

As the resolution is increased, the frequency sensitivity is improved because each bin of the FFT results in a smaller range of frequencies. The sampling rate is also increased, which improves the ability to distinguish between closely spaced frequency components. This is particularly important in coaxial networks where there can be multiple frequency components that are closely spaced. The ability to detect

these components allows for more fine-grained analysis of the discrete impedance characteristics often found in our cable access networks.

It is shown that tiny amplitude ripples can be detected in the frequency domain, some as small as 1/10th dB (Figure 21) and better. This graph shows a frequency domain chart on the left, having at least four dominant wave components that are superimposed. The smallest ripple can be seen at different places in the graph, with the example circled in red at the 679.6 MHz marker. In the time domain chart on the right, the contributing echo can be isolated in the impulse response.

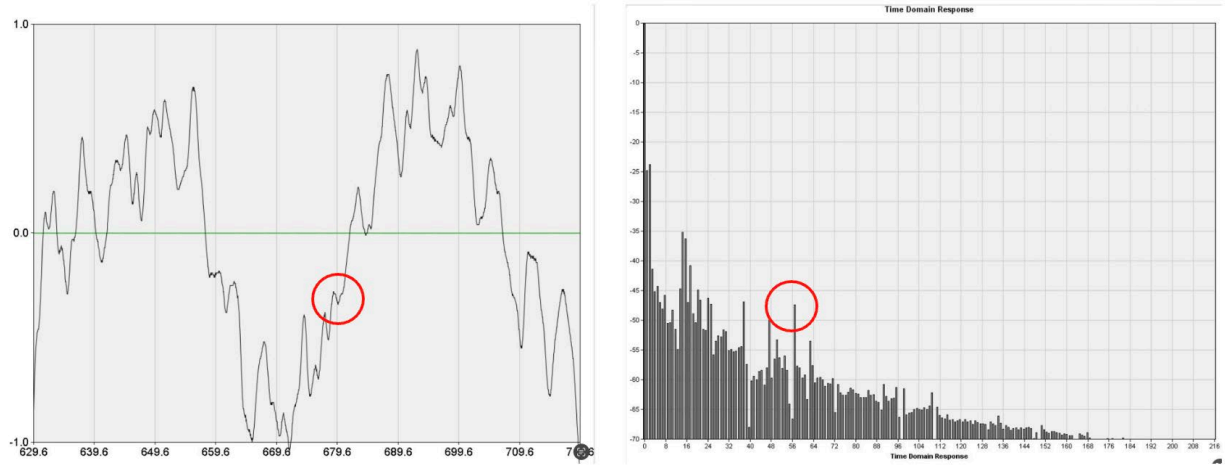

Figure 21 – Time and Frequency Domain Sensitivity

5.3. Determining Open Circuit vs. Short Circuit Faults

Figure 22 through Figure 25 were originally published by Larry Wolcott in PNM presentations from 2013 [10]. Many environments have recurring problems with certain types of faults such as water flooding, lightning strikes, construction damage, animal chews, damaged or missing terminators, and countless other issues.

A metallic time domain reflectometer (TDR) is a common diagnostic tool for testing and measuring coaxial cables. TDR tools used in the field transmit a defined width pulse and measure the time delay(s) of the reflections. When the time delays are used together with the propagational properties of the cable, precise distances of the impedance mismatches, faults and lengths can be calculated by the TDR. One of the unique and useful functions of a field TDR is that their displays typically show a distinctive raised (up) sweep for open circuit and inverted (down) sweep for short circuit faults. This feature can be useful for troubleshooting because it helps technicians better understand the nature of the fault.

Here are some examples of how a technician might interpret the information:

- Missing or damaged terminators show as open circuit.
- Radial and other cracks usually show as open circuit.
- Cracked cable that is moving (wind) may alternate between open circuit and short circuit.
- Buried cable with a ding should show a short circuit.

- Water flooded cable would show repeating short circuits.
- Connector or seizure problems could show as open circuit or short circuit.
  Example: The result may indicate a short circuit if the pin is touching or it may show an open circuit if the seizure is loose.

The TDR measures pulse responses which are a direct measurement of time delay. The OFDM channel estimates and OFDMA pre-equalization are built up from steady-state response to a long-lasting signal, and not an actual pulse response or a direct measurement of time delay.

The DOCSIS pre-equalization and channel estimates can provide similar information based on the same principles that are used by the field TDRs. This function is achieved by evaluating the phase of the echoes (impulse response) relative to the phase of the main tap, or DC term. Figure 22 shows three examples of impulse response on a coaxial transmission line. The top example shows an ideal response with no impedance mismatches, resulting in a relatively flat phase vs. frequency response. The middle example shows a short circuit reflection with the phase vs. frequency graph having a negative or downward slope (red arrow). Lastly, the lower illustration depicts an open circuit fault where the echo is more positive or upward (red arrow), indicating an in-phase reflection.

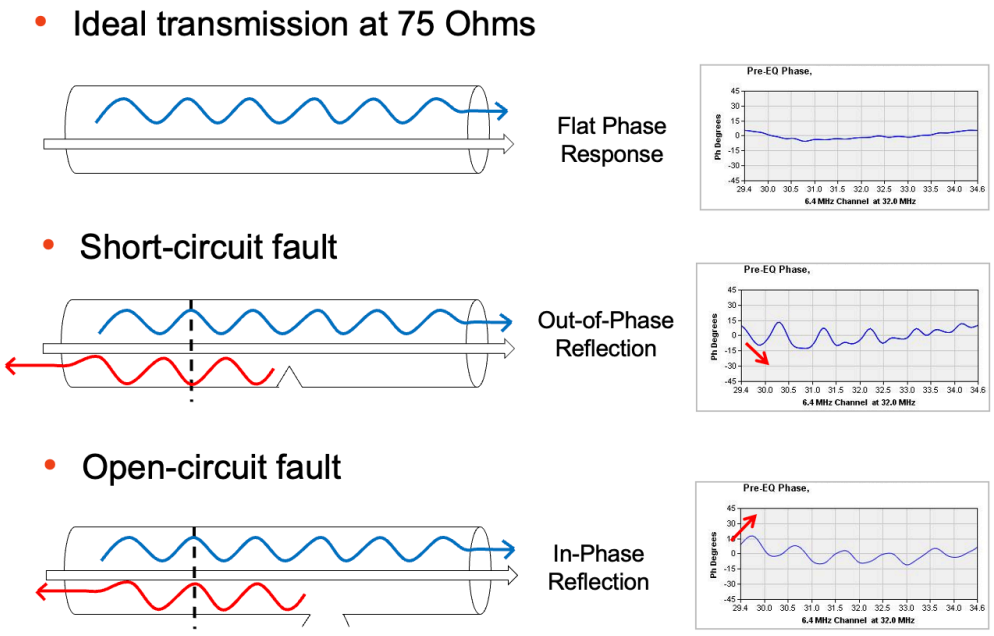

Figure 22 – Open Circuit vs. Short Circuit Reflections

Phase is a component of our signal that most of the other test results (tools) can't provide. This phase is part of the quadrature constellation and can be measured in degrees. Zero degrees from the equalizer's perspective means "in phase" if the coefficients have been corrected. Without correction (having linear delay), the echo impulse having the same relative phase as the main tap component is the same as "in phase." Figure 23 and Figure 24 show a phasor with positions of 0 degrees and 180 degrees in red.

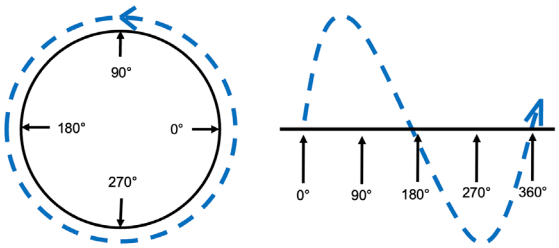

Figure 23 – Phase Polar (left) vs. Wave (right) Displays

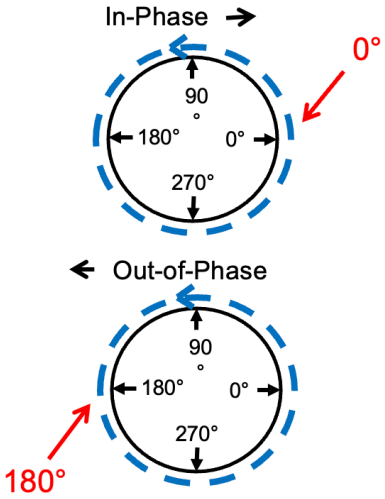

Figure 24 – Echo Phase Rotations Relative to Main Tap Phase

Figure 25 shows a comparison of a cut drop cable, unterminated on the left and soaking in a solution of saturated salt water on the right. The saline solution is highly conductive and a reliable way to produce a short circuit response the resembles something typically seen in the field. The impulse response of each echo contains a phase value, demonstrating that the technique continues to work for OFDM and OFDMA coefficient analysis.

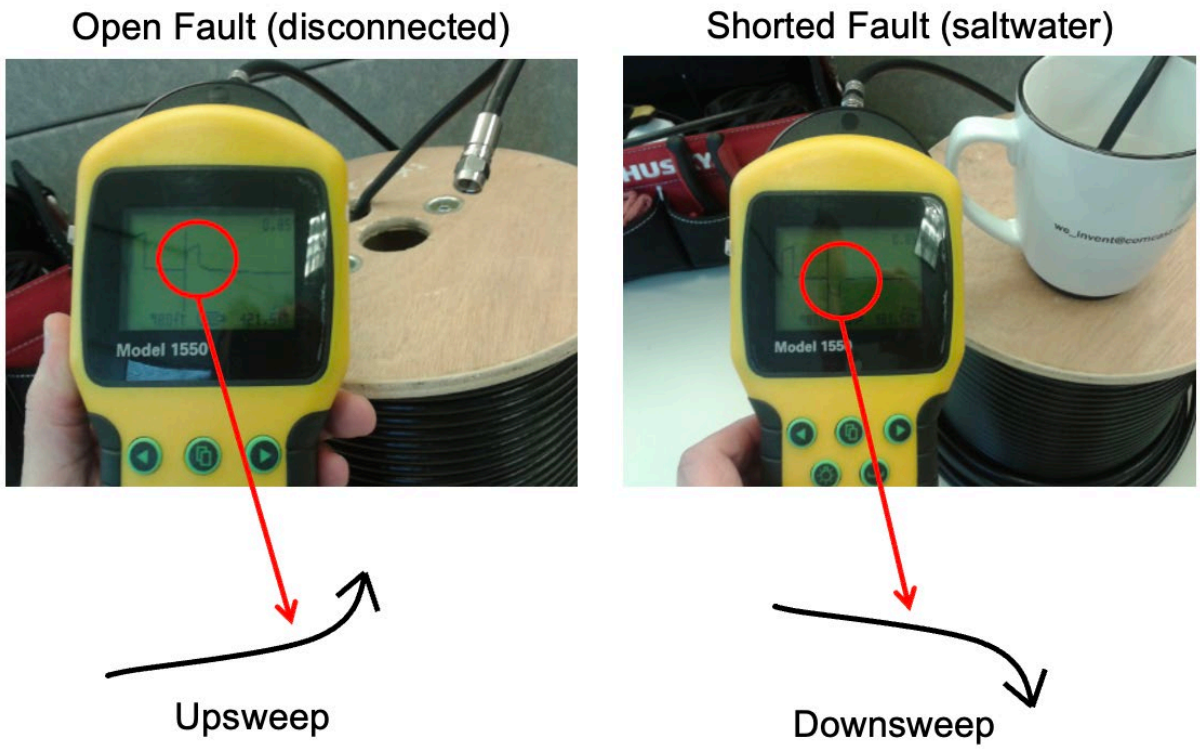

Figure 25 – Open Circuit vs. Short Circuit TDR Response

Multiple echoes that superimpose causes complications because of the constructive and destructive properties of the signal. If there are multiple echoes at the same time, two or more sharing the same phase and amplitude will be additive or increase in size. If more than one echo exists at the same time with opposing phase and amplitude, they will cancel each other. When examining a single cable in the field with a TDR, this isn't usually a problem because there is only one path for the signal to traverse. However, with a connected plant containing splitters, couplers and taps, there are multiple paths for the TDR's test signal and as such, increases the risk of echo responses that overlap.

The PNM community has largely agreed to avoid using direct references to TDRs to avoid confusion caused by similarities, with significant differences in the way the tools are used and interpreted. It's important to reinforce here that the echo distances are a measurement of the length of an impedance cavity. The distances relative to the CM location, for example, are unrelated. To say that differently, it is usually incorrect to say, "the distance from the cable modem."

5.4. Cyclic Prefix Tuning

DOCSIS 3.1 and 4.0 OFDM and OFDMA employ a technique of copying and prepending a portion of the symbol called the cyclic prefix (CP). The CP is used to mitigate the effects of reflections within the channels, which can result in inter-symbol interference (ISI). The CP is very effective but comes at the expense of capacity within the channel because of the unusable time allocated to the CP. By default, a typical DOCSIS system might use a CP length of 2.5 microseconds, for example. In the case of a 96 MHz wide downstream OFDM channel using 50 kHz subcarrier spacing, assuming a CP value of 512

(2.5 microseconds), this results in an additional impact of 88.89% to the symbol efficiency. (DOCSIS OFDM efficiency calculations are addressed in SCTE 270 2021r1, Mathematics of Cable [11].)

Using the PNM adaptive pre-equalization coefficients and OFDM channel estimates offers a valuable tool for observation of the (approximate) channel performance including reflected energy and phase response. In both cases, the frequency domain estimates of the channel can be converted to the time domain using the IFFT. This time domain representation offers an excellent analysis of the echoes present within the channel, which may require mitigation using the CP. Figure 26 illustrates the overlaid impulse responses of an entire service group containing thousands of CMs.

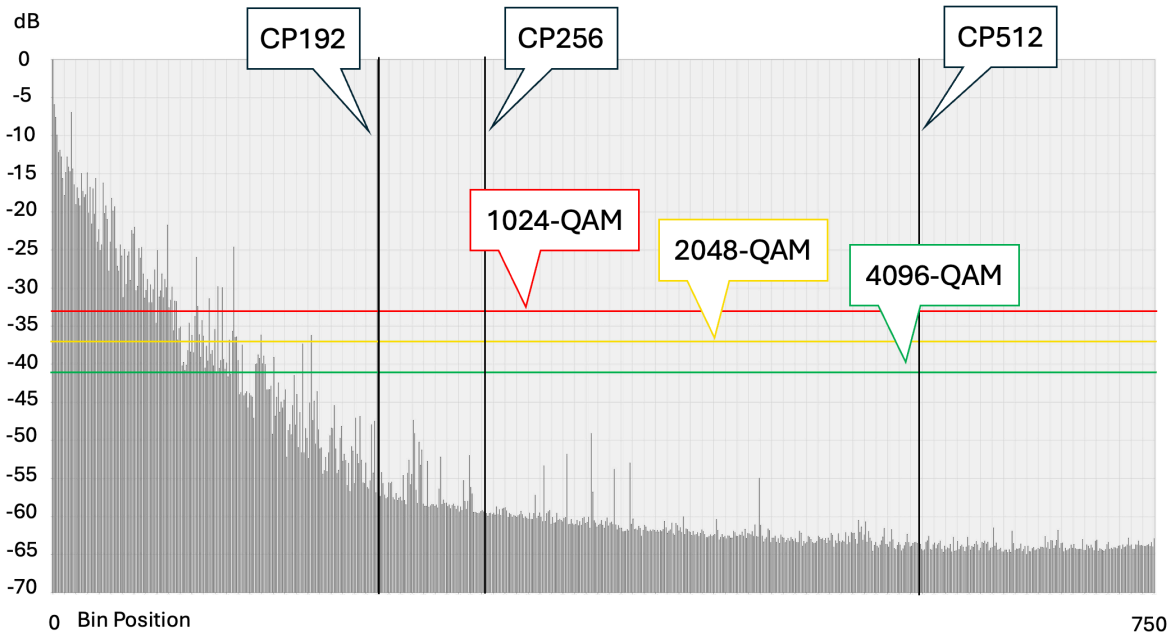

Figure 26 – OFDM Time Domain Impulse Response

The zero position (farthest left) of the graph represents the incident signal at the receiver and OFDM channel estimate's time domain bins extending to the right. The horizontal markers represent 1024-QAM, 2048-QAM and 4096-QAM RxMER thresholds. These thresholds were taken from the DOCSIS 3.1 PHY specification [4], and are 34 dB, 37 dB and 41 dB respectively. The vertical markers represent the time-equivalent of the indicated CP values, 192, 256 and 512. These are 0.9375 microseconds, 1.25 microseconds and 2.5 microseconds, respectively.

In this example, none of the CMs in the population of this analysis require a CP greater than 256 because the total integrated power of the bins is well within the desired operational requirements of 4096-QAM. Thus, the CP value can be reduced from 512 to 256, or 2.5 microseconds to 1.25 microseconds respectively. In the case of a 96 MHz wide downstream OFDM channel using 50 kHz subcarrier spacing, assuming a CP value of 256, this results in a contribution of 94.12% to the symbol efficiency. This CP reduction results in a total improvement of 5.23% symbol efficiency within the channel. This is free bandwidth.

5.5. Detecting Cable Lengths

Unlike the predecessor PNM implementations using the limited SC-QAM pre-equalization coefficients and full band capture analysis, the improved resolution and sensitivity brings new opportunities to analyzing the network. Considering that the sensitivity is good enough to measure impedance cavities

from subtle impedance mismatches, this technique can be useful for measuring unimpaired cables. For example, the differences in impedance between the drop cable and tap port, along with the outlet cable and input port at the modem can be measured. Likewise, splitters, ground blocks and home amplifiers all have imperfect impedance characteristics.

For an OFDM channel with 104.5 MHz of contiguous active subcarriers, the time domain of the channel estimate is displayed in Figure 27; there are at least four dominant echoes seen in the impulse response. The impulse response graph on the left of the figure shows each of the echoes circled in red with a label showing the number of delay bins separating the main tap, 2, 15, 39 and 59 respectively. The middle section of the figure shows the frequency domain waveform of each echo when isolated as a discrete component. Finally on the right, the frequency response shows the superposition of all four waves including all components.

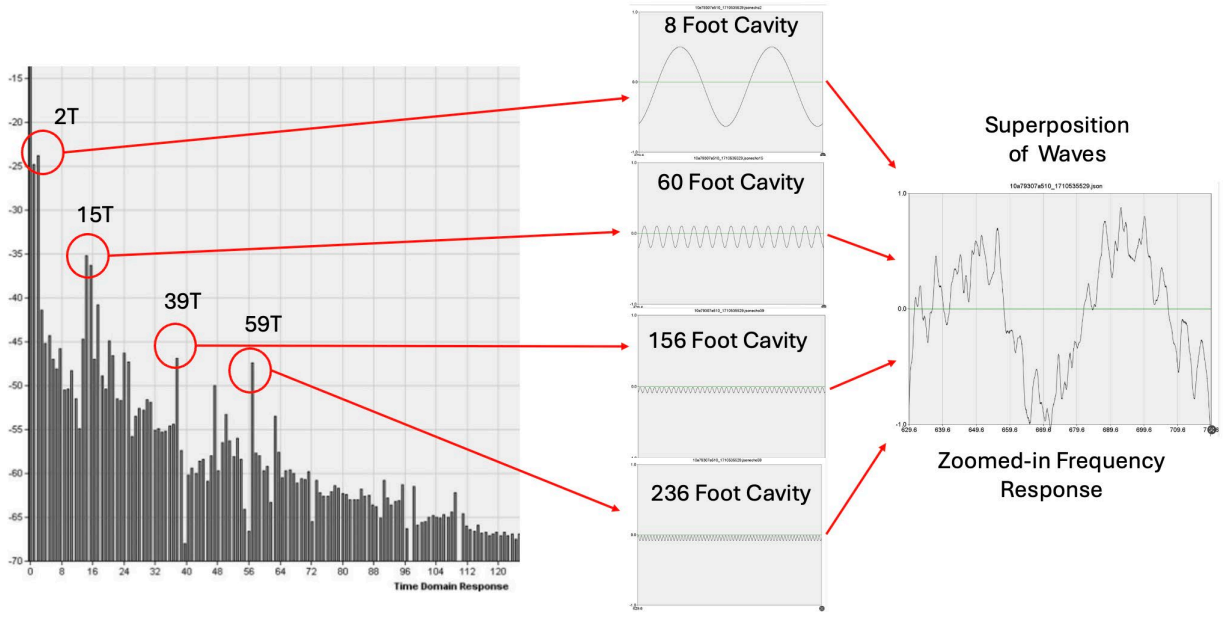

Figure 27 – Superposition of Four Constituent Amplitude Ripples

This technique allows the distances of the cable interconnections to be measured in some cases. This is especially true when the impedances deviate significantly from 75 ohms. Figure 28 shows a coaxial topology starting with the CM on the left, connected to the outlet with an 8 ft jumper, then 60 ft of wiring to a ground block, 156 ft of drop cable to the tap, then 236 ft of feeder to the line amplifier. Knowing the width of the contiguous active subcarriers for OFDM channel (96 MHz in this case) and math described in section 4.4.1, each of the cable lengths matches perfectly with the constituent wave components identified in Figure 27. This technique has several promising applications for automating cable network topology discovery. These concepts are explored further by Lin Cheng and co-authors in their paper "Exploring Programmatically Generated HFC Plant Topology" [12].

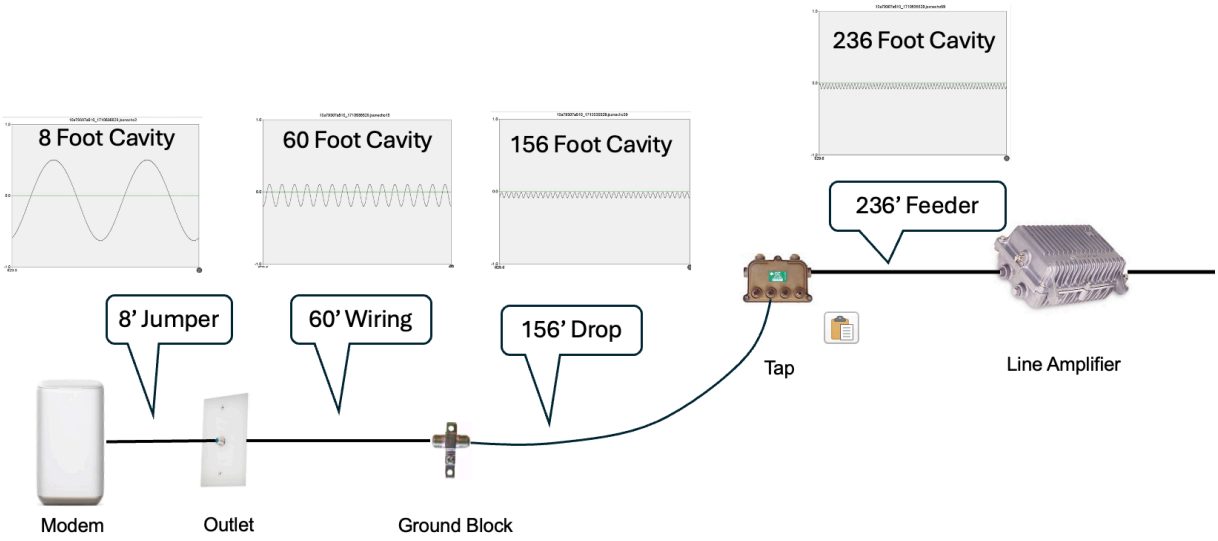

Figure 28 – Coaxial Interconnection Distances and Reflection Cavities

6. Field Results

The PNM community has been discussing the topic of enhanced resolution and sensitivity in OFDM on DOCSIS networks for several years. This paper continues to evaluate the theories and ideas surrounding these enhancements. From our previous decade of PNM experience, we know that nothing is truly validated until it is proven in the field. These trials represent some of the first real-world tests of these advanced PNM capabilities, marking a significant step in their practical implementation. Two of the most common PNM troubleshooting scenarios are examined, although there are many more which could be explored for further benefit.

6.1. Cracked trunk cable, causing egress (leakage) and ingress

A trunk cable was discovered to have a crack in the outside shielding, which was causing a leak. The leak was detected with calibrated leakage equipment attached to a network maintenance truck. Figure 29 shows a red X on the topology map with multiple dot clusters. Dot colors represent unimpaired service in blue and errors detected in the others. The red circle in the photograph (right) is the approximate location of the radial crack. This cable is suspended over a river, beyond the reach of a typical bucket lift, requiring specialized repair equipment.

Figure 29 – Cracked Aerial Cable on Side of Bridge

Figure 30 illustrates another map view of the CM population, relative to the cracked cable which is marked with a red X in the middle. The green FBC spectrum display on the left is associated with the population of blue dots, which are unaffected by FM ingress. The spectrum region of 88 MHz to 108 MHz is circled in green, showing a flat noise floor. The display on the right outlined in red is representative of the population on the other side of the cable fault, with dots that are not blue. The red circle shows the frequency spectrum of 88 MHz to 108 MHz with a spike in the noise floor, consistent with FM ingress that is typical with ingress entering the plant at the radial crack.

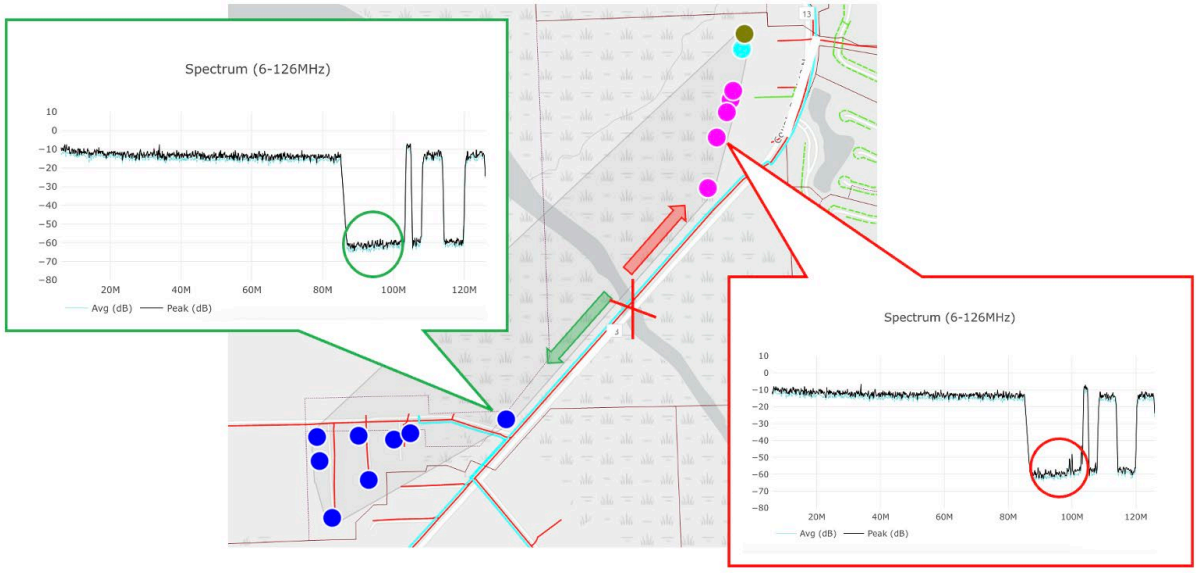

Figure 30 – Small Amounts of FM Ingress Visible in FBC Beyond the Damage

The traditional PNM techniques based on SC-QAM pre-equalization coefficients continue to perform as expected. Figure 31 is like Figure 30 with the cracked cable marked by a red X. The green bordered display on the left side of the marked fault shows a flat frequency response. The display on the right side of the marked fault (downstream) shoes a 9T echo in the upstream pre-equalizer response. As these SC-QAM channels are configured, this indicates an impedance cavity of approximately 795 feet, with 85 feet of potential error.

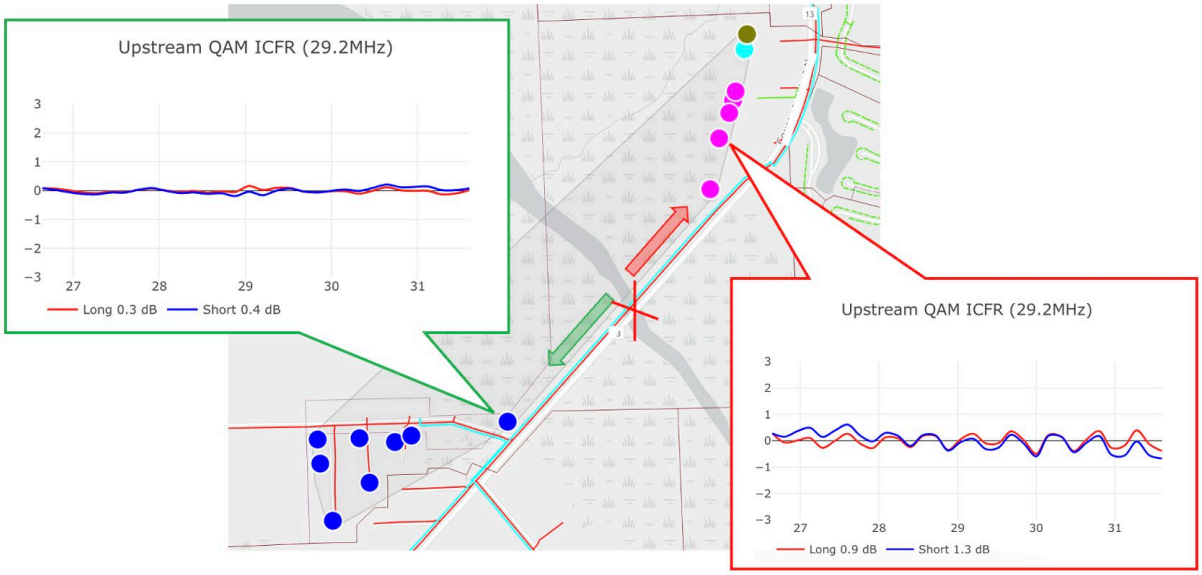

Figure 31 – 9T Reflection (~1dB) in SC-QAM Upstream Pre-EQ Response

When examining the downstream OFDM channel estimates, the impulse response appears more precise, showing much greater detail with at least six dominant echoes. Compared to the limited bandwidth and resolution of the SC-QAM pre-equalizer response, the OFDM channel provides a dramatic improvement.

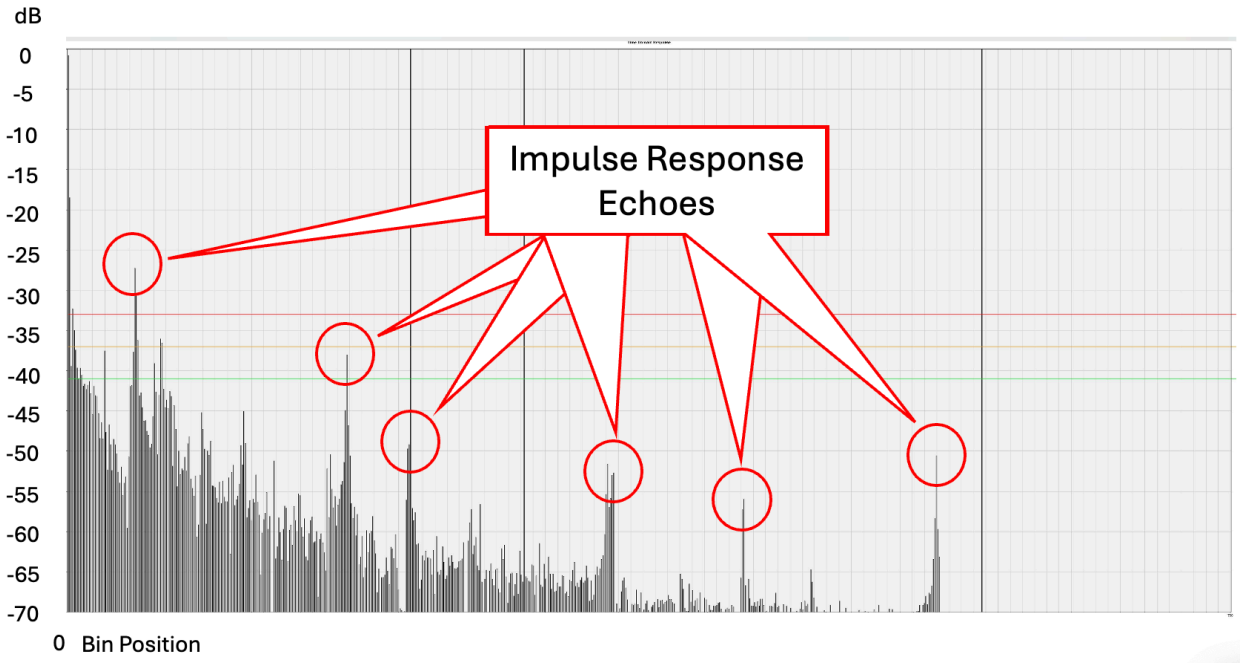

Figure 32 – Multiple Discrete Time Domain Echoes

6.2. Loose connector with egress (leakage) and ingress

Identifying loose connectors was one of PNM's earliest successes. Does the new enhanced capability add value to the existing PNM technology and techniques? By using the OFDM channel estimates, the current methods of equalizer response measurement and FM ingress detection can be implemented in a single operation. It is also possible that using them together can improve the reliability and confidence in the former detection method.

Loose connectors at the input to the CM have distinctive indicators. The FBC graph in Figure 33 shows a frequency spectrum that is occupied with downstream SC-QAM channels. High levels of ingress are circled in red with indicators of FM, very high frequency (VHF), ultra high frequency (UHF) and LTE at their respective frequencies. The first clue is the high levels of FM ingress, relative to the SC-QAM channels. This is often caused by the proximity of the ingress location to the receiver, very close to the loose connector at the input of the CM. In this case, there is very little attenuation of the FM ingress, compared to several hundred feet of coaxial cable.

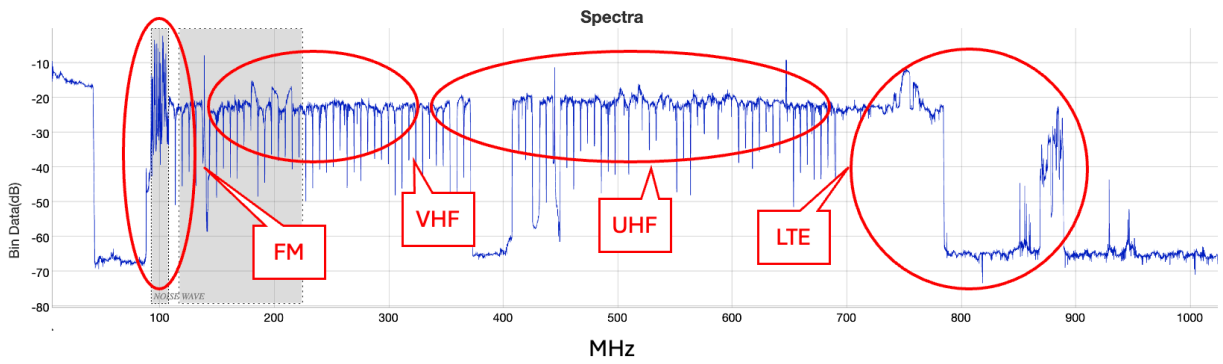

Figure 33 – FBC from 6 MHz to 1026 MHz Showing Example of Spectrum Affected by a Loose Connector, Allowing Significant Ingress

The OFDM channel estimates show LTE ingress circled in red when looking at the frequency domain amplitudes (Figure 34). This same information is confirmed with the FBC chart in Figure 33. A similar result would be expected from the downstream RxMER per subcarrier PNM test, so it's not clear that much additional insight would be gained using the new technique.

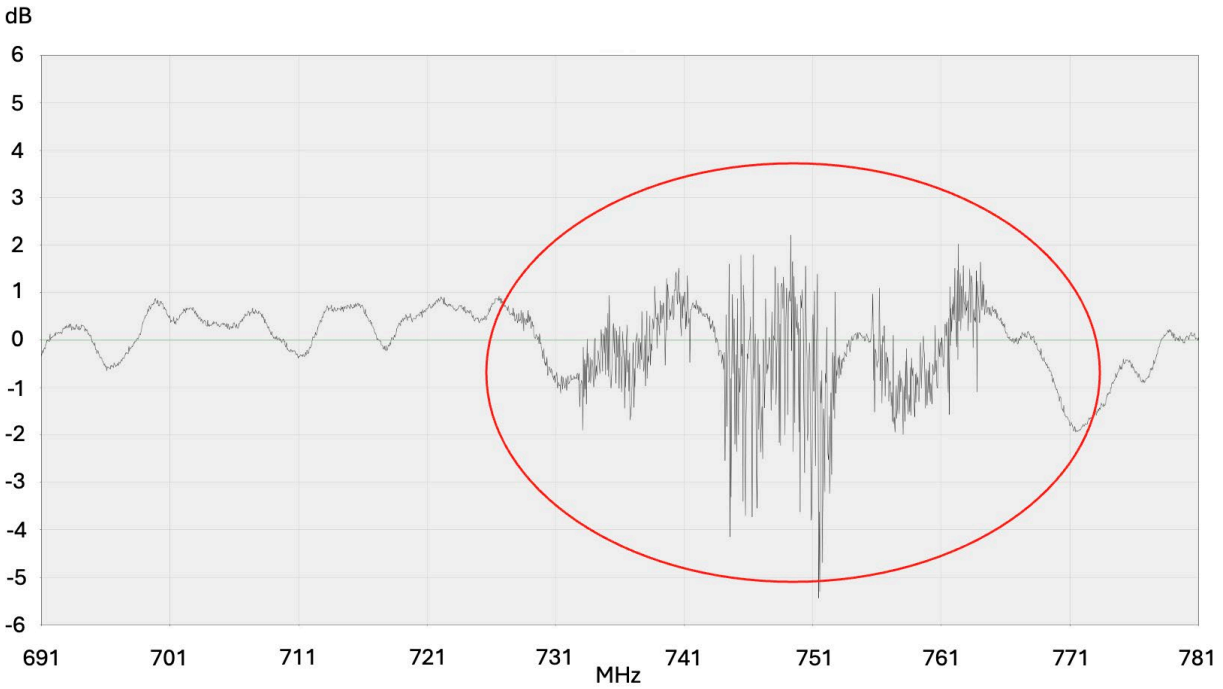

Figure 34 – LTE Interference in the OFDMA Channel Estimates

7. Conclusion

In this paper, we took the observations and methods reported by Tom Williams et al [1] and demonstrated several modifications for important use cases, for PNM and more. By applying the correction methods

where needed, localization is greatly improved through more precise matching of pre-equalization and channel estimation results, and through more accurate calculations of the distances to impedance mismatches. Due to the large amounts of data obtainable from channel estimation and pre-equalization data from OFDM and OFDMA respectively, greater accuracy in distance estimation is possible. While work continues to develop repeatable methods for finding and localizing some complex faults in coax plant, early results are promising. But one simple and important use case we have demonstrated here is to verify entire large populations of CMs where the CP can be reduced, thus adding more bandwidth for use on the cable plant.

Appendix A

8. Decoding

8.1. CmDsOfdmChanEstimateCoef Decoding Details

The downstream OFDM channel estimate files can be decoded using the file format specified in Table 63 – Channel Estimate Coefficient File Format of [5] in section D 2.6. The following pseudo-code reads the channel estimate file in the correct order and byte lengths:

```
channelEstimate.setFileType(readFileType(dataInputStream)); // read 4 bytes
channelEstimate.setFileVersion(readFileVersion(dataInputStream)); // read 1 + 1 byte
channelEstimate.setTimestamp(readFileTimestamp(dataInputStream)); // read 4 bytes
channelEstimate.setDsChannelId(readChannelId(dataInputStream)); // read 1 byte
channelEstimate.setMacString(readMacString(dataInputStream)); // read 6 bytes
channelEstimate.setSubcarrierZeroFreq(dataInputStream.readInt()); // read 4 bytes
channelEstimate.setFirstActiveSubcarrierIndex(dataInputStream.readShort()); // read 2 bytes
channelEstimate.setSubcarrierSpacing(dataInputStream.readByte()); // read 1 byte
channelEstimate.setFilesize(dataInputStream.readInt()); // read 4 bytes
channelEstimate.setIqValues(readIQValues(dataInputStream, channelEstimate.getFilesize()));
```

Note that the I and Q values are manipulated from s2.13 format to accommodate the target language. In this example, the language is Java floating point:

```
short iComponentRaw = dataInputStream.readShort();
int iComponent = iComponentRaw << 3 >> 3; // Sign-extend to 32 bits and shift right to get 16-bit signed integer
short qComponentRaw = dataInputStream.readShort();
int qComponent = qComponentRaw << 3 >> 3; // Sign-extend to 32 bits and shift right to get 16-bit signed integer

// Divide by 2^13 (s2.13 format)
float iFloat = iComponent / 8192.0f; // 8192.0 = 2^13
float qFloat = qComponent / 8192.0f; // 8192.0 = 2^13
```

This pseudo-code ensures that the channel estimate file is read correctly, and the I and Q values are properly converted from their s2.13 format to floating point values in Java.

8.2. CmUsPreEq Decoding Details

The upstream OFDMA pre-equalization files can be decoded using the file format specified in Table 77 - Last PreEqualization Update File Format from [5], in section D.13. The I and Q values should be scaled and processed in a similar manner as described in Section 8.1. Note that there are differences in the number format: s2.13 and s2.14 are used in the two operations (as specified).

. The following pseudo-code reads the channel estimate file in the correct order and byte lengths:

```
preEqCoefficients.setFileType(readFileType(dataInputStream)); // read 4 bytes
preEqCoefficients.setFileVersion(readFileVersion(dataInputStream)); // read 1 + 1 byte
preEqCoefficients.setTimestamp(readFileTimestamp(dataInputStream)); // read 4 bytes
preEqCoefficients.setUsChannelId(readChannelId(dataInputStream)); // read 1 byte
preEqCoefficients.setMacString(readMacString(dataInputStream)); // read 6 bytes
preEqCoefficients.setCmtsMacString(readMacString(dataInputStream)); // read 6 bytes
preEqCoefficients.setSubcarrierZeroFreq(dataInputStream.readInt());// read 4 bytes
preEqCoefficients.setFirstActiveSubcarrierIndex(dataInputStream.readShort());// read 2 bytes
preEqCoefficients.setSubcarrierSpacing(dataInputStream.readByte());// read 1 byte
preEqCoefficients.setFilesize(dataInputStream.readInt());// read 4 bytes
preEqCoefficients.setIqValues(readIQValues(dataInputStream, preEqCoefficients.getFilesize()));
```

The I and Q values should be scaled and processed in a similar manner as described in Section 8.1. Note that there are differences in the number format: s2.13 and s2.14 are used in the two operations (as specified).

Abbreviations

CCAP	converged cable access platform
CM	cable modem
CMTS	cable modem termination system
CP	cyclic prefix
dB	decibel
dBmV	decibel millivolt
DC	direct current
DOCSIS	Data-Over-Cable Service Interface Specifications
DS	downstream
DSP	digital signal processing
EQ	equalizer
ENBW	equivalent noise bandwidth
FBC	full band capture
FD	frequency domain
FFT	fast Fourier transform
FIR	finite impulse response
FM	frequency modulation
ft	foot or feet
Hz	hertz
I	in-phase
IFFT	inverse fast Fourier transform
kHz	kilohertz
MAC	media access control
MAP	bandwidth allocation map
MIB	management information base
MHz	megahertz
ns	nanosecond
OFDM	orthogonal frequency-division multiplexing
OFDMA	orthogonal frequency-division multiple access
PNM	proactive network maintenance
Pre-EQ	pre-equalization
Q	quadrature
QAM	quadrature amplitude modulation
RBW	resolution bandwidth
RF	radio frequency
RNG-RSP	ranging response
RxMER	receive modulation error ratio
SC-QAM	single carrier quadrature amplitude modulation
SCTE	Society of Cable Telecommunications Engineers
SNMP	Simple Network Management Protocol
TDR	time domain reflectometer
TFTP	Trivial File Transfer Protocol
UHF	ultra high frequency
US	upstream
VHF	very high frequency
VoP	velocity of propagation

Bibliography & References

[1] OFDMA Predistortion Coefficient and OFDM Channel Estimation Decoding and Analysis Remove the linear delay, examine the group delay, Tom Williams et al, SCTE Cable-Tec Expo 2021

[2] PNM Best Practices: HFC Networks (DOCSIS® 3.0) CM-GL-PNMP-V03-160725, July 25, 2016, Cable Television Laboratories, Inc.

[3] Data-Over-Cable Service Interface Specifications DOCSIS® 3.1, DOCS-IF3-MIB-2024-07-05, July 5, 2024, Cable Television Laboratories, Inc.

[4] DOCSIS® 3.1 Physical Layer Specification CM-SP-PHYv3.1-I20-230419

[5] Data-Over-Cable Service Interface Specifications DOCSIS® 3.1 Cable Modem Operations Support System Interface Specification, CM-SP-CM-OSSIv3.1-I26-240615

[6] Data-Over-Cable Service Interface Specifications DOCSIS® 3.1, CCAP™ Operations Support System Interface Specification, CM-SP-CCAP-OSSIv3.1-I27-231012

[7] A Comprehensive Case Study of Proactive Network Maintenance, Heslip, Thomas, Gonsalves, Wolcott, SCTE Cable-Tec Expo 2016

[8] Pre-Equalization Based Upstream Frequency Response Measurements, SCTE NOS WG7 (Note: At the time this paper was written, the listed reference document was undergoing final review and editing.)

[9] Understanding and Troubleshooting Cable Upstream RF Spectrum, SCTE NOS WG7 (Note: At the time this paper was written, the listed reference document was in the approval process.)

[10] Scout Flux eTDR Open vs. Short, Larry Wolcott, Comcast PNM Presentation, 2013

[11] SCTE 270 2021r1 Mathematics of Cable

[12] Exploring Programmatically Generated HFC Plant Topology (2023), Cheng, Campos, Riggert and Wolcott, SCTE Cable-Tec Expo 2023

